Faculty of Science

CEITEC MOTES

Stable Co(II) Single-Ion Magnets for Thermal Evaporation Deposition

Ivan Nemec [a,b]

[a] *Department of Inorganic Chemistry, Faculty of Science, Palacký University, Olomouc, CZ*
[b] *Magneto-Optical and THz Spectroscopy, CEITEC Brno University of Technology, Brno, CZ*

IAP Meeting 2023, Benguerir

Faculty of Science,
Palacky University
Olomouc

Department of Inorganic Chemistry

Synthesis of coordination compounds
Molecular Magnetism
X-ray diffraction lab

Central European Institute of Technology,
Brno University of Technology
Brno

Magneto-Optical and THz Spectroscopy (RGL: Neugebauer)
HFHF-EPR, FIRMS

Synthesis of coordination compounds, organic radicals
Thin films of molecular compounds

Magnetism in nanoworld

- upon decreasing particle size of the magnetic materials to nm dimensions new phenomena arise
- superparamagnetism: no domain structure, large fluctuating magnetic moments
- energy barrier to spin reversal, blocking temperature (T_B) $f(T_B) = (KV, \tau)$

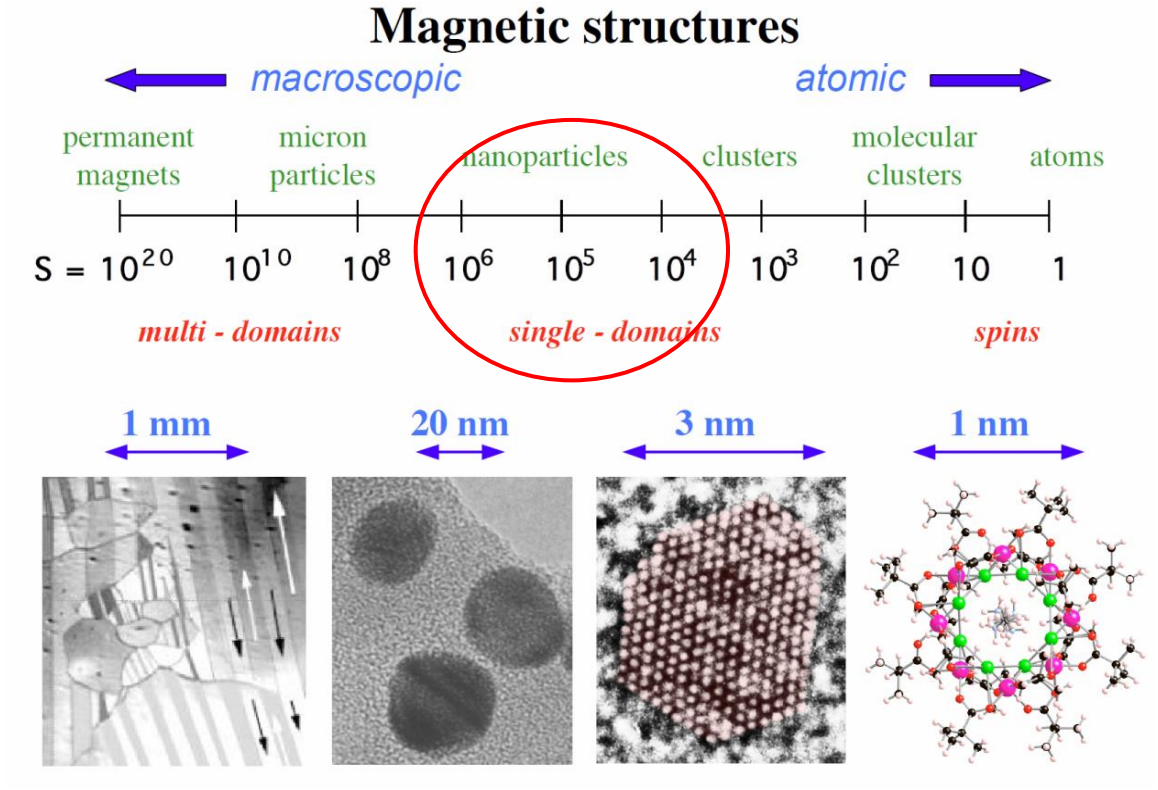

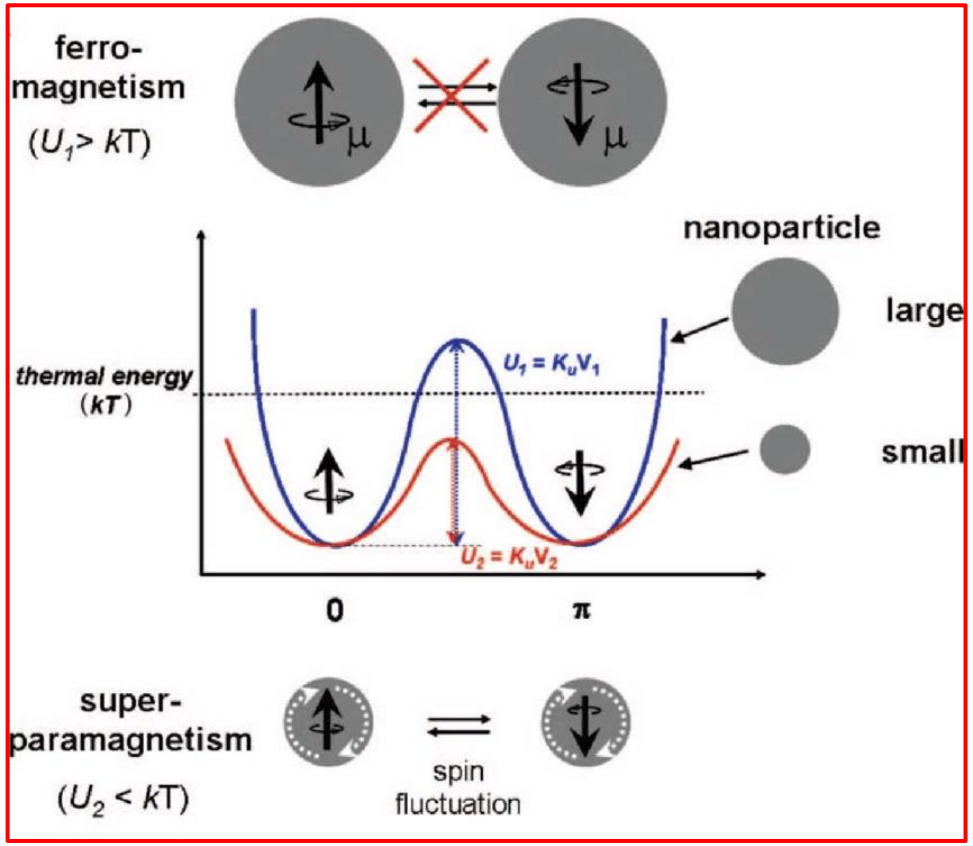

W. Wernsdorfer et al. *Coord. Chem. Rev.*, **2021**, 213984

Magnetism in nanoworld: Single Molecule Magnets

- when the size is decreased to individual molecules, similar phenomenon to SP could be observed, individual molecules can behave as nanomagnets
- fingerprint: slow relaxation of magnetization thanks to existence of energy barrier (*U*)
- *U* depends on magnetic anisotropy parameters (*D*) of the ground spin state (*S*), *D* < 0 (axial anisotropy)

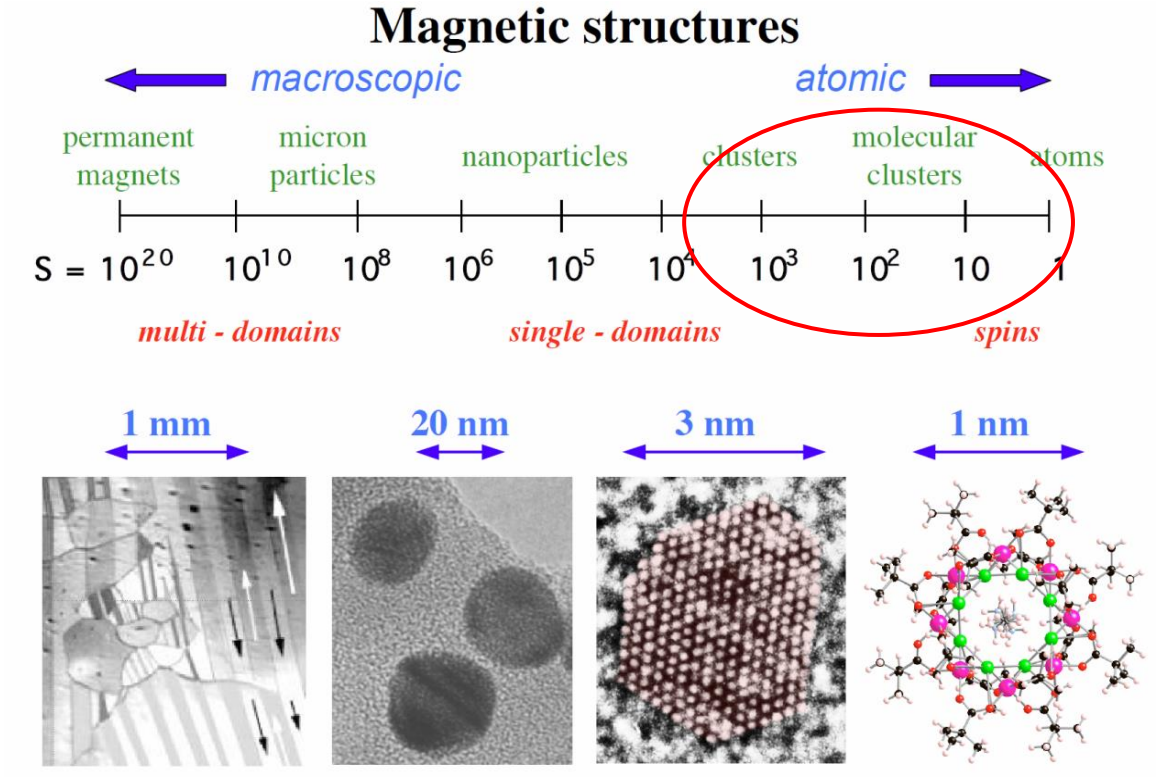

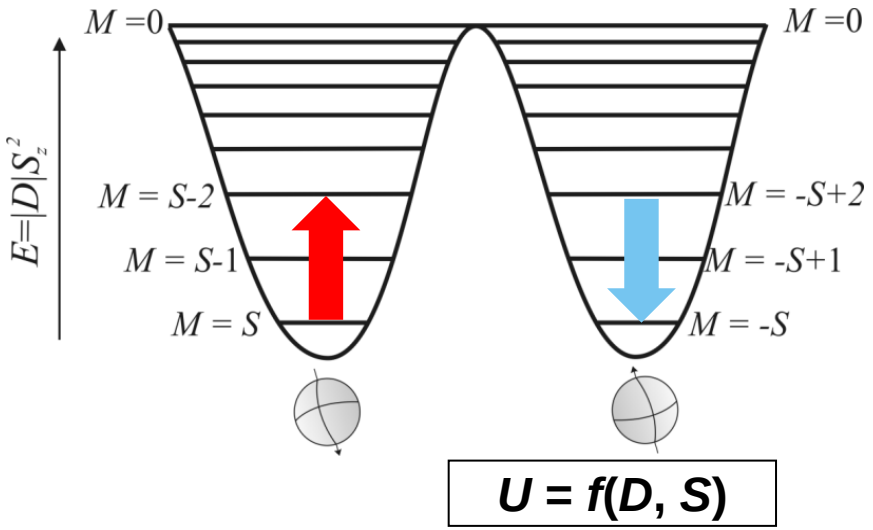

$U = f(D, S)$

Integer spins $U = |D|S^2$
or
Half-integer $U = |D|(S^2\text{-}1/4)$

Very rare situation, usually $U_{eff} << U$

W. Wernsdorfer et al. *Coord. Chem. Rev.*, **2021**, 213984

Single Molecule Magnets

- Relaxation of magnetization can occur via diverse pathways:

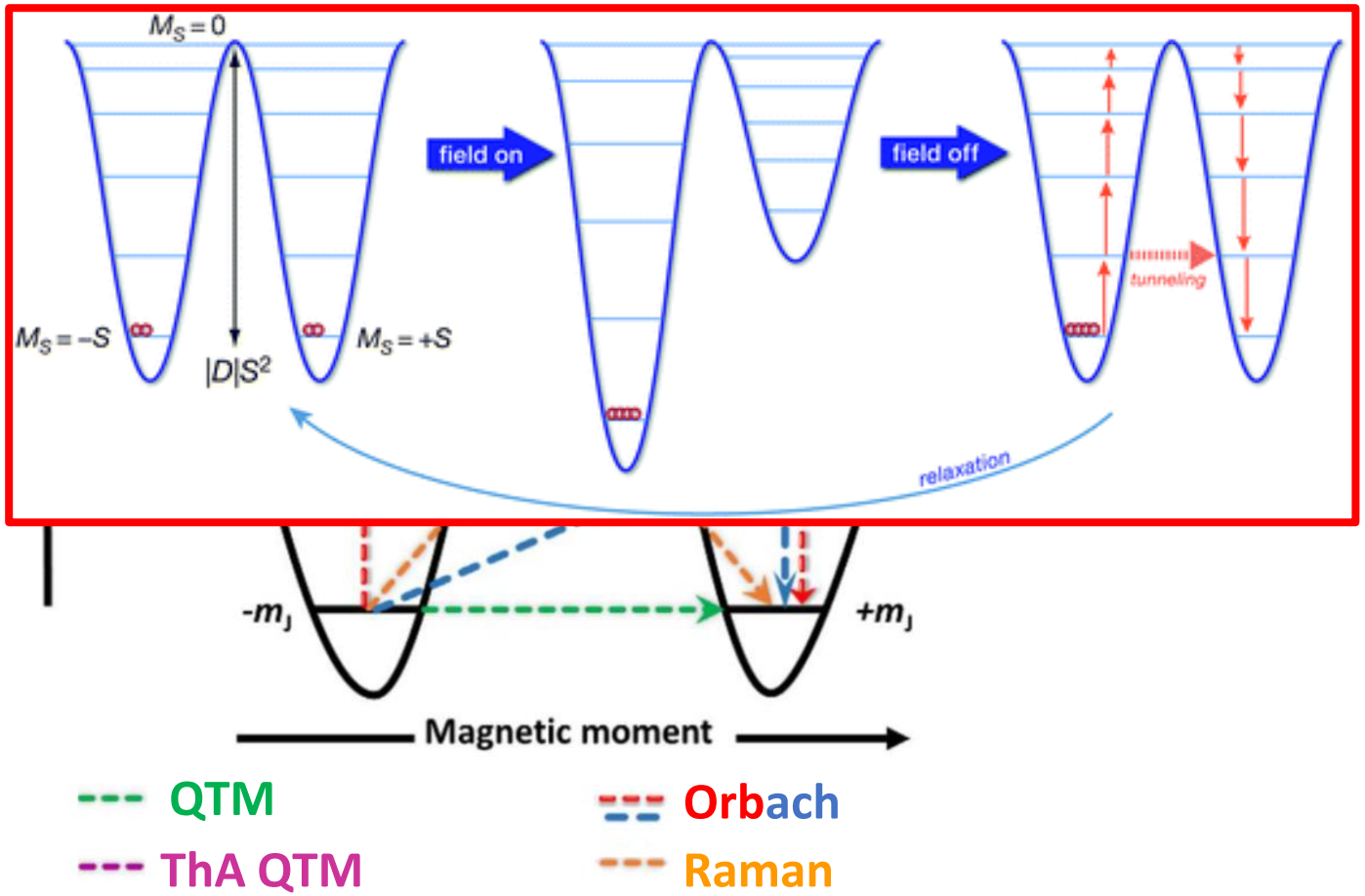

Direct process – single phonon process involving the phonons with the same energy as the magnetic resonance quantum *hv* - spin to flip without traversing the energy barrier, τ^{-1} shows the ΔT and dc applied field dependence.

Raman process - two-phonon process with the scattering of phonons - phonon frequencies are related to each other by $h(v2 - v1) = \Delta$, leading to the strong ΔT dependence, but the non-dependence on *B*.

Orbach process - direct, resonant two-phonon process via a real intermediate state - two phonons related to each other by $h(v2 - v1) = \Delta$.

Quantum tunneling – through the barrier. Can be hindered by the static magnetic field = Field Induced SMMs

E. Colacio et al. *Coord. Chem. Rev.*, **2021**, 213984

Single Molecule Magnets

- design of new SMMs based on tuning *D* and not increasing *S* – Single Ion Magnets (SIMs)
- increase of T_B up to temperature of liquid nitrogen

from SMMs to SIMs

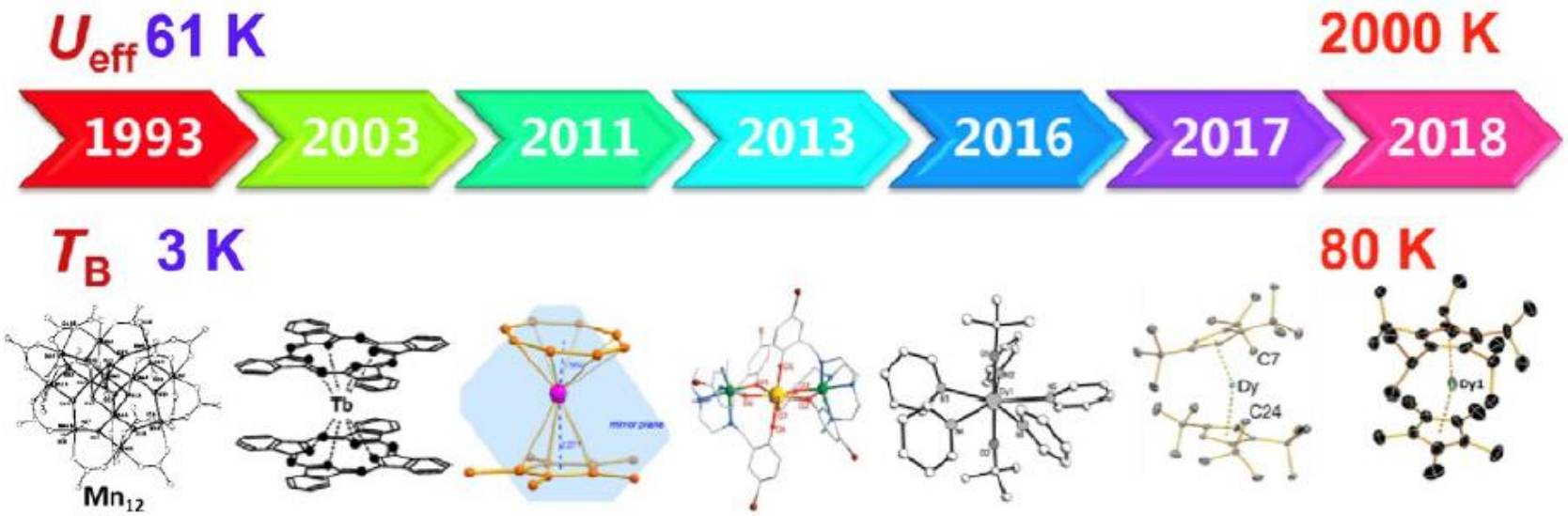

Molecular magnetic hysteresis at 60 kelvin in dysprosocenium

CAP Goodwin et al. *Nature*, **2017**, 548, 439

Magnetic hysteresis up to 80 kelvin in a dysprosium metallocene single-molecule magnet

Fu-Sheng Guo et al. *Science*, **2018**, 362, 1400

SMMs methods of investigation

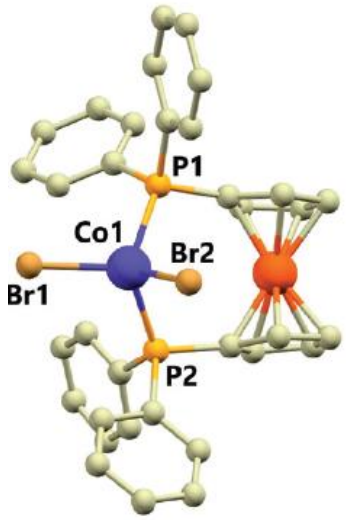

DC magnetometry

$$\hat{H} = D\left(\hat{S}_z^2 - \hat{S}^2/3\right) + E\left(\hat{S}_x^2 - \hat{S}_y^2\right) + \mu_B B g \hat{S}_a$$

$$M_{\mathrm{mol}} = 1/4\pi \int_0^{2\pi} \int_0^{\pi} M_a \sin\theta d\theta d\varphi$$

$|E/D| = 0 - 1/3$

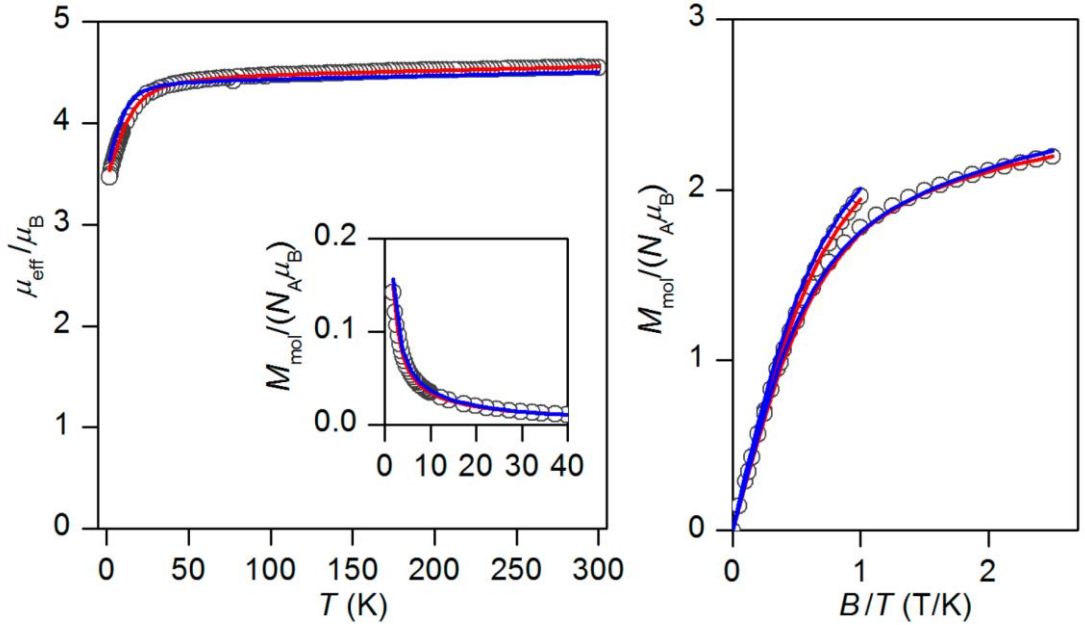

HF-EPR

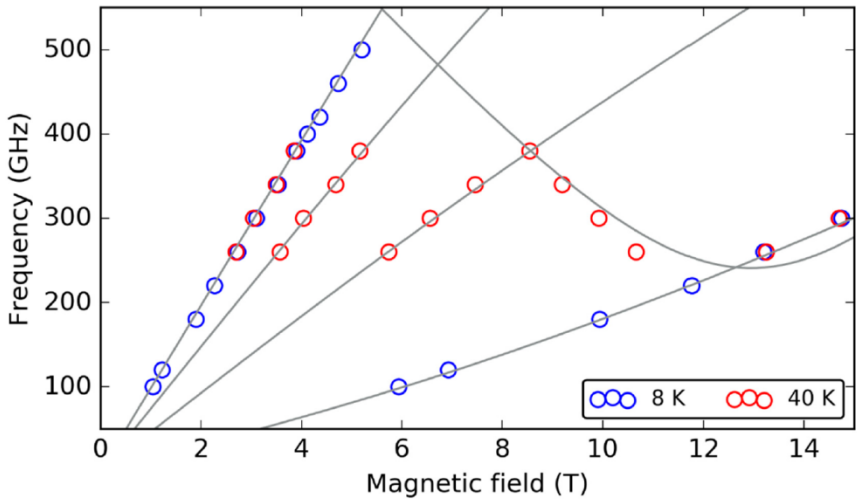

Sign of *D*

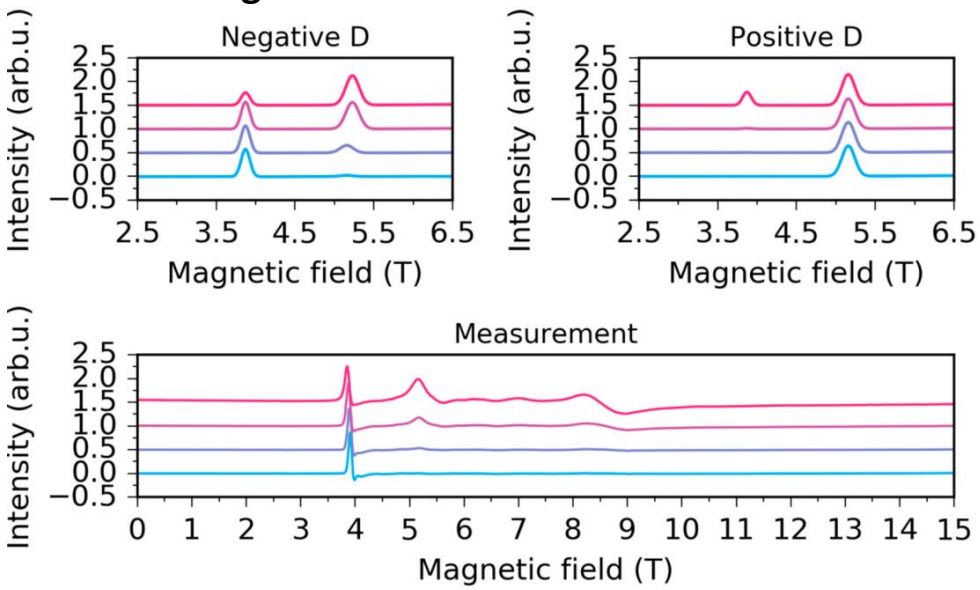

J. Hruby *et. al. Dalton Trans.* **2020**, 49, 11697

SMMs methods of investigation

- study of relaxation processes, analysis of AC magnetic data (AC magnetic field ~4Oe):
- Real (χ') and imaginary (χ'') components fitted

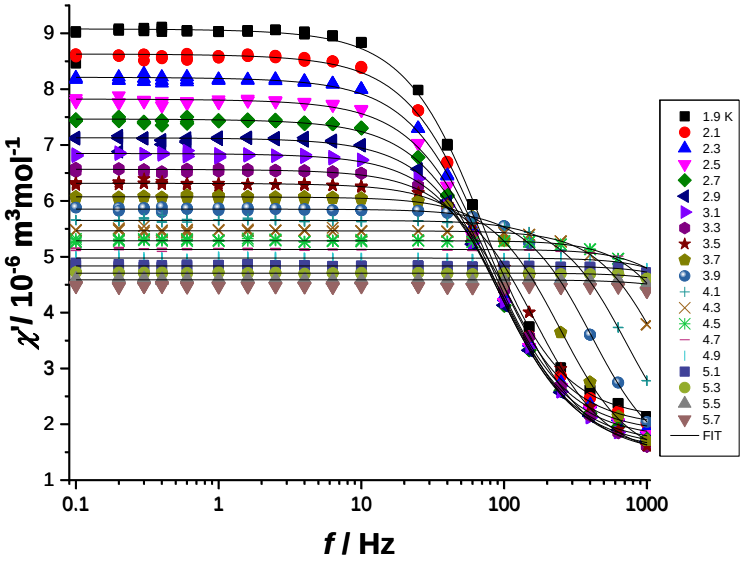

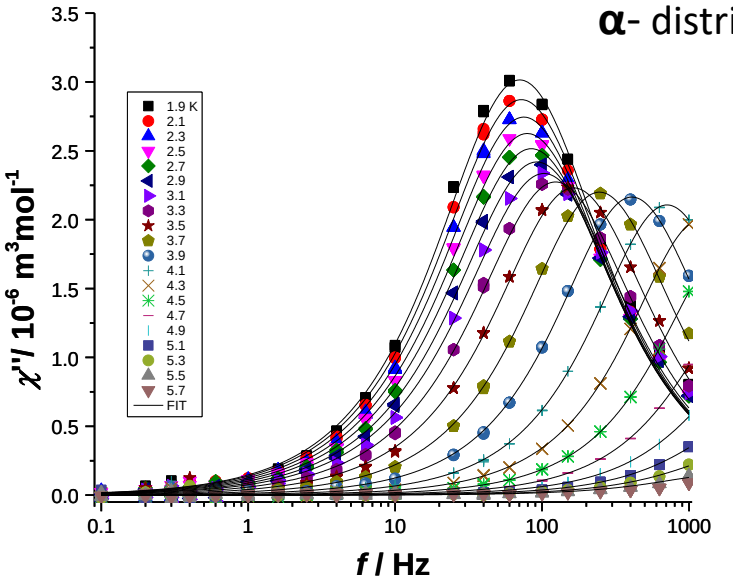

χ_T- thermodynamic susceptibility, χ_S – adiabatic susceptibility

α- distribution of relaxation times, **τ – spin-lattice relaxation time**

$$\chi' = \chi_s + (\chi_T - \chi_s)\frac{1 + (\omega\tau)^{(1-\alpha)}\sin(\frac{\pi\alpha}{2})}{1 + 2(\omega\tau)^{(1-\alpha)}\sin\left(\frac{\pi\alpha}{2}\right) + (\omega\tau)^{(2-2\alpha)}}$$

$$\chi'' = (\chi_T - \chi_s)\frac{(\omega\tau)^{(1-\alpha)}\cos(\frac{\pi\alpha}{2})}{1 + 2(\omega\tau)^{(1-\alpha)}\sin\left(\frac{\pi\alpha}{2}\right) + (\omega\tau)^{(2-2\alpha)}}$$

$$\tau^{-1} = \tau_0^{-1}\exp\left(-\frac{U_{\text{eff}}}{k_B T}\right) + CT^n + AH^m T + c_0$$

$$= \tau_0^{-1}\exp\left(-\frac{U_{\text{eff}}}{k_B T}\right) + d\left(\frac{1+eH^2}{1+fH^2}\right)T^n + AH^m T + \left(\frac{b_1}{1+b_2H^2}\right)$$

Orbach Raman direct QT

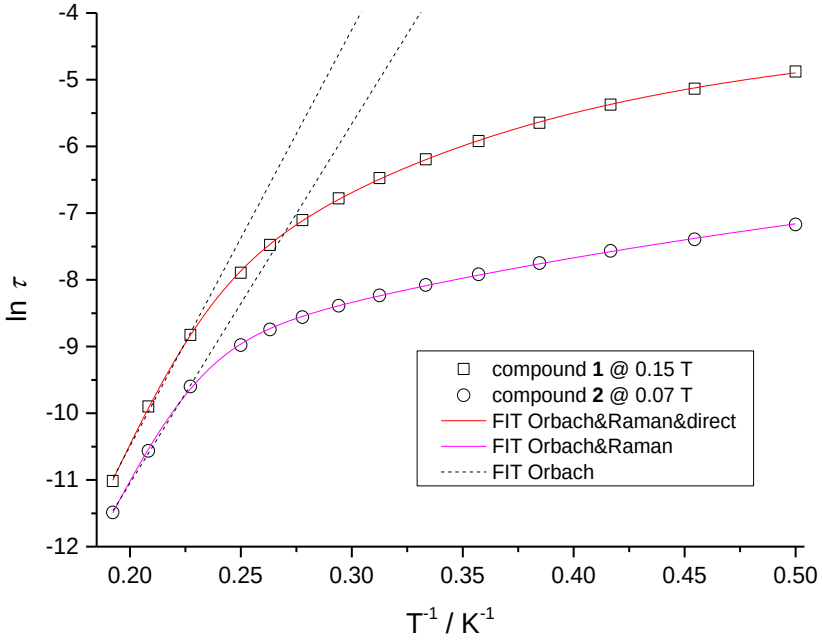

Single Molecule Magnets

Theoretical investigations
CASSCF/NEVPT2 calculations

Values of zero-field splitting parameters, g-tensor, Kramers doublets…

Electronic structure – ligand field terms
AILFT module – splitting of d-orbitals

SINGLE_ANISO module
Probabilities of relaxation mechanisms

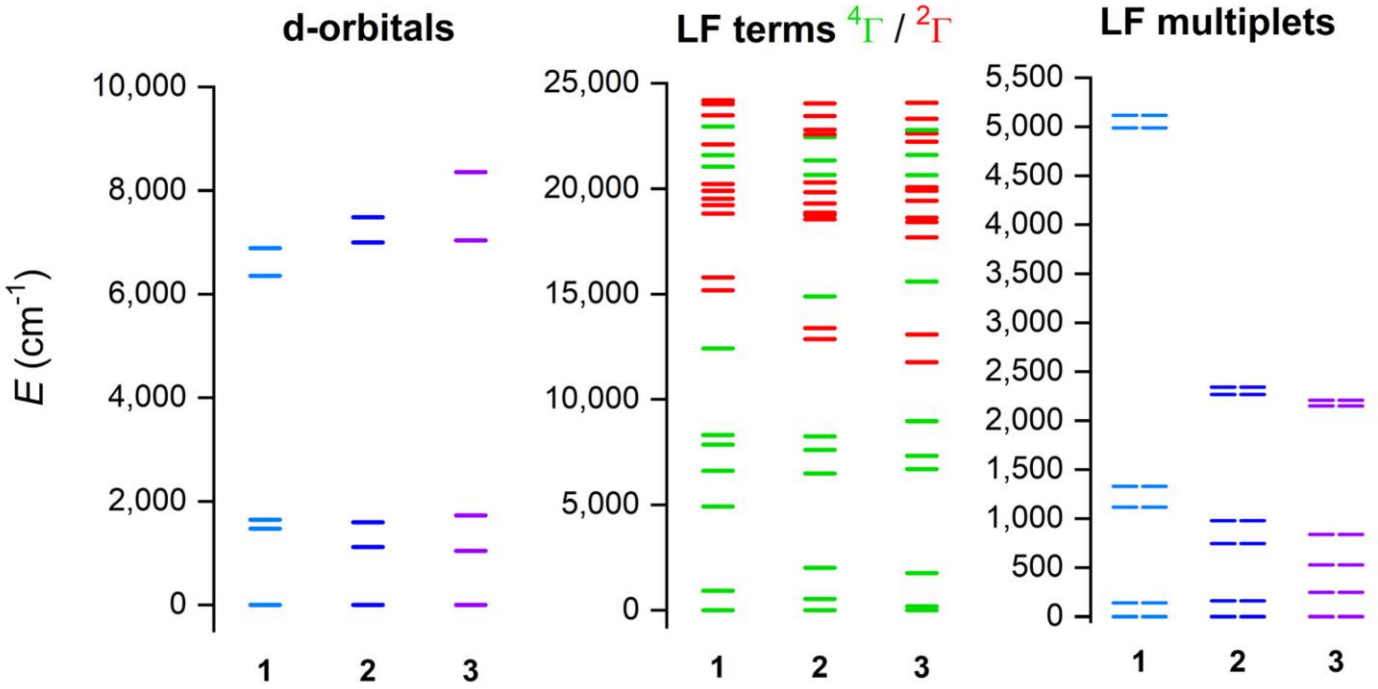

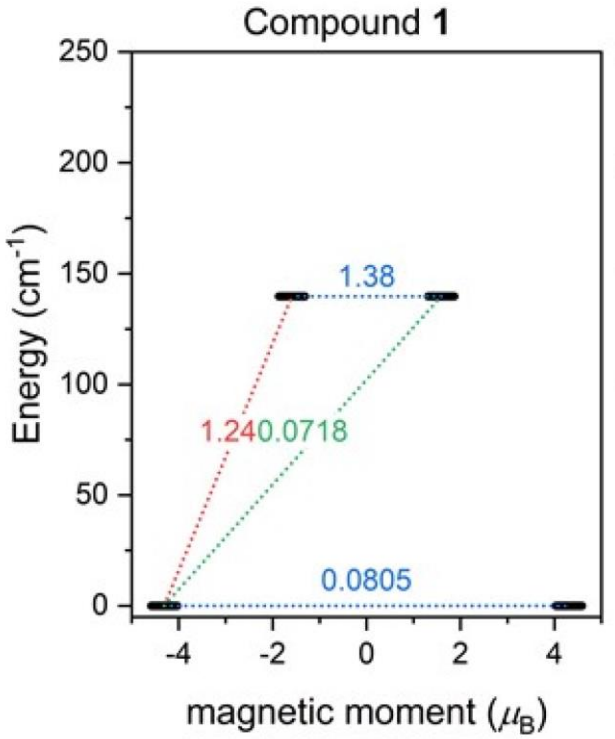

Malmqvist, P.Å.; Roos, B.O. Chem. Phys. Lett. **1989**, 155, 189–194.
Angeli, C et al. Chem. Phys. Lett. **2001**, 350, 297–305.

L.F. Chibotaru et al. J. Phys. Chem. **2012**, 137, 064112.

Used computational methods

- All DFT and CASSCF/NEVPT2 calculations (n-electron valence state perturbation theory) were performed using ORCA 4.2 computational package [1]
- Coordinates from X-ray diffraction experiments were used as inputs for single-point DFT at B3LYP (def2-TZVP) level. Hirshfeld atom refinements (HAR) using NoSpherA2 module in Olex2 1.5 [2] at B3LYP (def2-SVP or def2-TZVPD) level were used for obtaining final structural file.
- All geometry optimization was done by DFT at B3LYP (def2-TZVP) level including D3BJ dispersion correction
- Geometry optimization of the selected molecular fragments were done by DFT at B3LYP (def2-TZVP) level
- Calculations of ZFS parameters were done using CASSCF/NEVPT2 calculations. Active space was set to five d-orbitals of Co(II), {CAS (7,5) , *S* = 3/2, 10 quartet and 40 doublet roots)
- QTAIM calculations were performed using MultiWFN software [3]
- Topology of coordination polyhedra was determined calculating continuous shape measures (CSMs) using SHAPE 2.1 software [4]

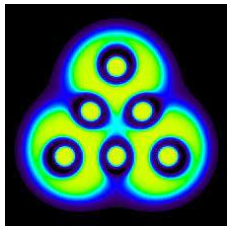

[1] (a) F. Neese, *Rev.: Comput. Mol. Sci*., **2012**, 2, 73–78;
(b) F. Neese, *Rev.: Comput. Mol. Sci*., **2018**, 8, e1327.
[2] (a) O.V Dolomanov *et al*. *J. Appl. Cryst*., **2009**, 42, 339-341.;
(b) F. Kleemiss *et al*. *Chem. Sci*., **2021**,12, 1675-1692
[3] T. Lu and F. Chen. *J. Comput. Chem*., **2012**, 33, 580
[4] P. Alemany et al. *Rev. Comp. Chem*., **2017**, 30, 289

SMMs@surfaces

- For practical application of SMMs the deposition on functional (e.g. conductive, magnetic) surfaces is needed. This allows e.g. control, read-out etc.
- Problem with stability of the deposited SMMs – typically, the best SMMs are low coordinated species.
- Besides decomposition also changes in the molecular geometry, new phonon modes appear due surface
- Notable examples SMMs@surfaces: metallofullerenes

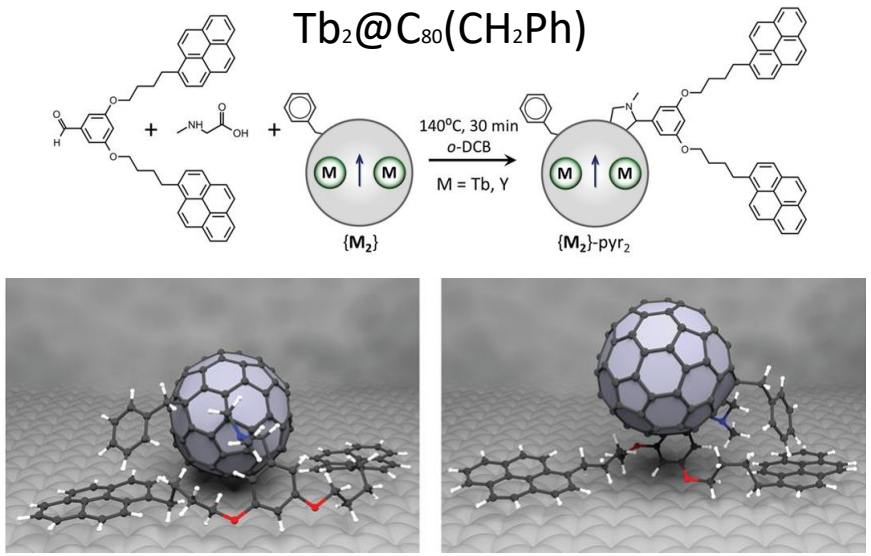

Non-trivial synthesis (electric arc) and purification

bulk

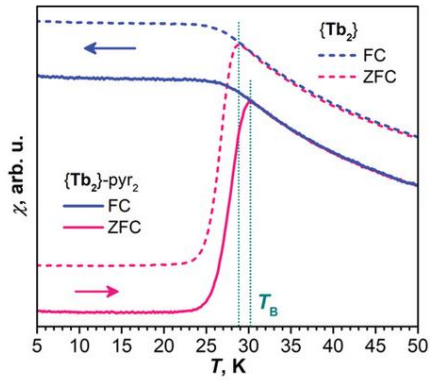

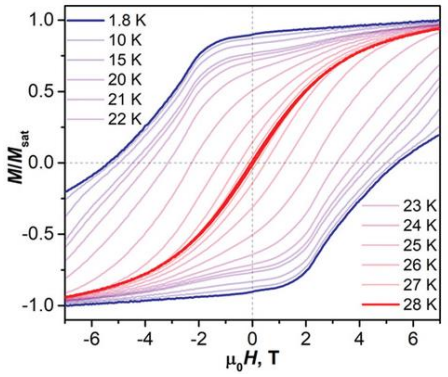

Sub monolayer

T_B = 28K

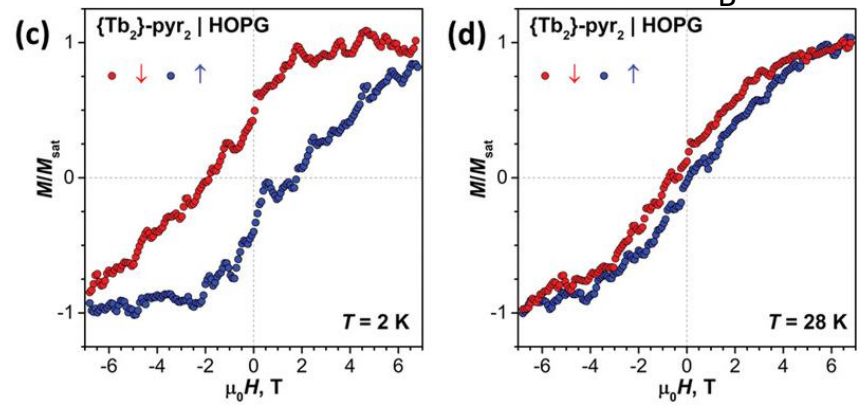

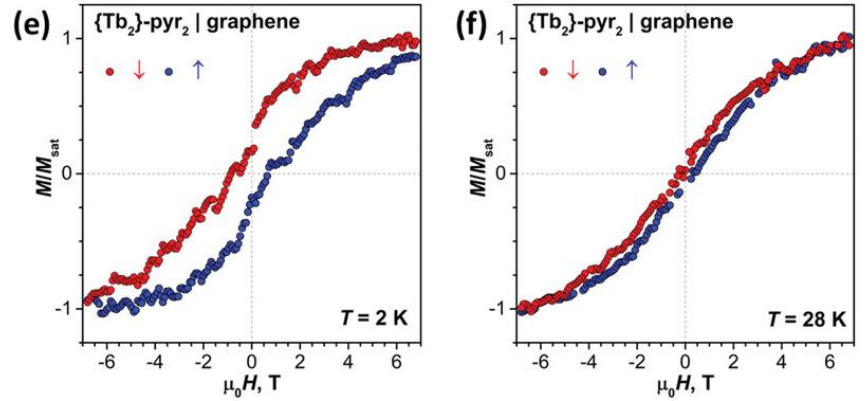

L. Spree et al. Adv. Funct. Materials, 2021, 31, 48, 105516

Tetra-coordinate Co(II) SMMs

- Easy synthesis, relatively good stability, interesting magnetic properties: tetra-coordinate Co(II) complexes
- Magnetic anisotropy is governed by symmetry of ligand field – typically angular distortions from T_d

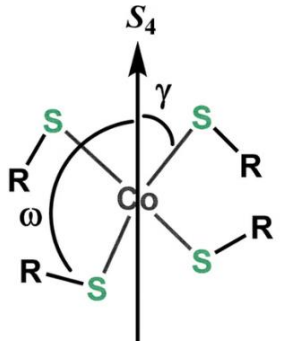

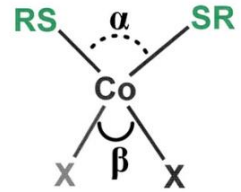

X = Cl, Br, I

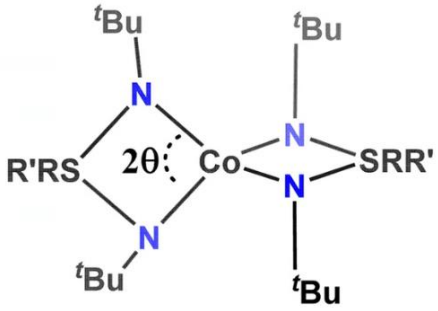

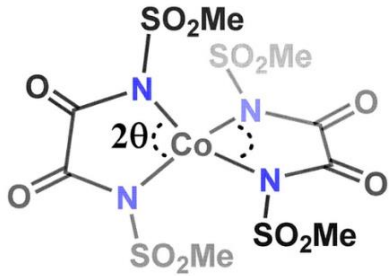

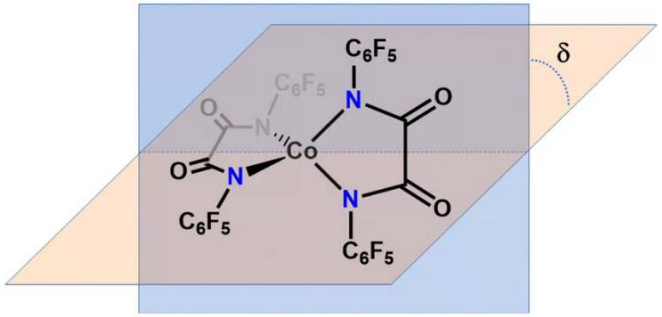

δ = dihedral angle between N-Co-N chelate planes

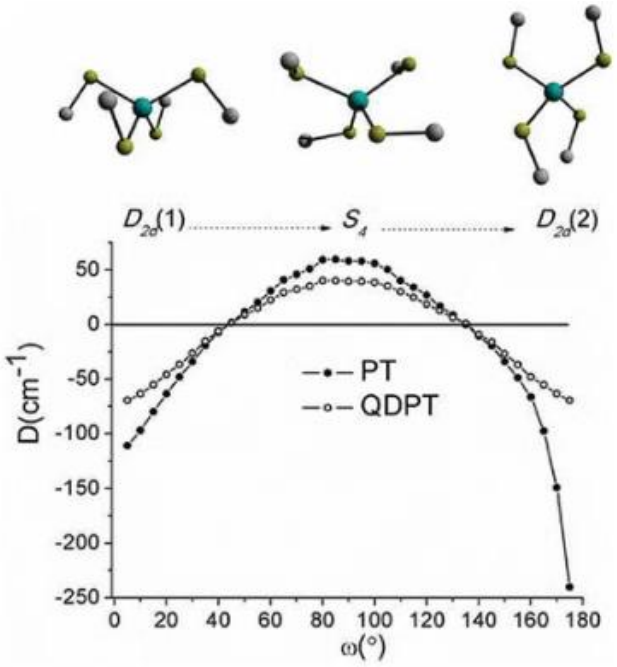

S Vaydia et al. *Inorg. Chem.*, **2016**, 9564

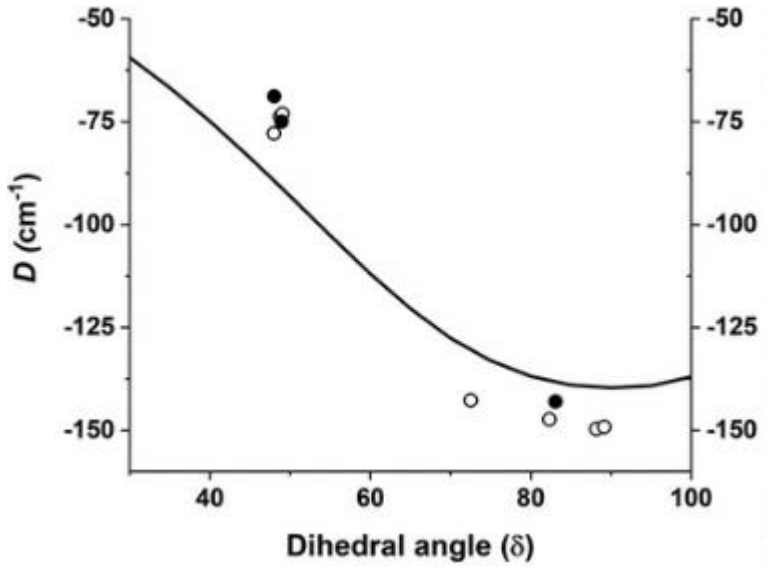

M Wang et al. *J.Sol. St. Chem.*, **2021**, 122209

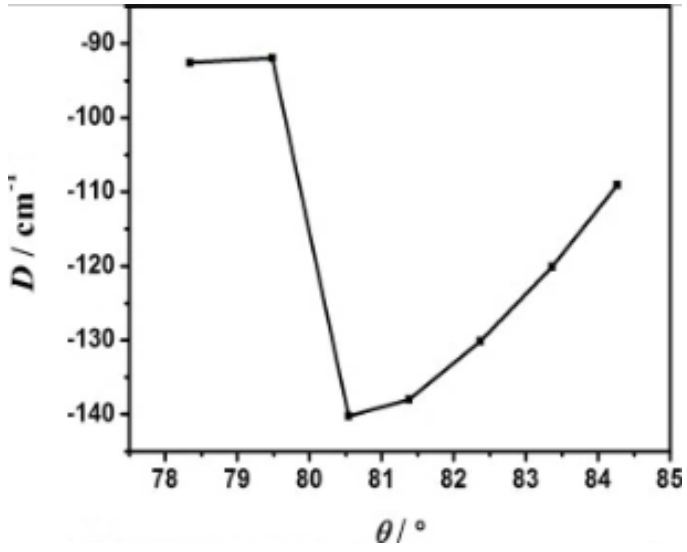

D Maganas et al. *Inorg. Chem.*, **2011**, 8741

Tetra-coordinate Co(II) SMMs

- Easy synthesis, relatively good stability, interesting magnetic properties: tetra-coordinate Co(II) complexes
- Magnetic anisotropy is governed by symmetry of ligand field – typically angular distortions from T_d

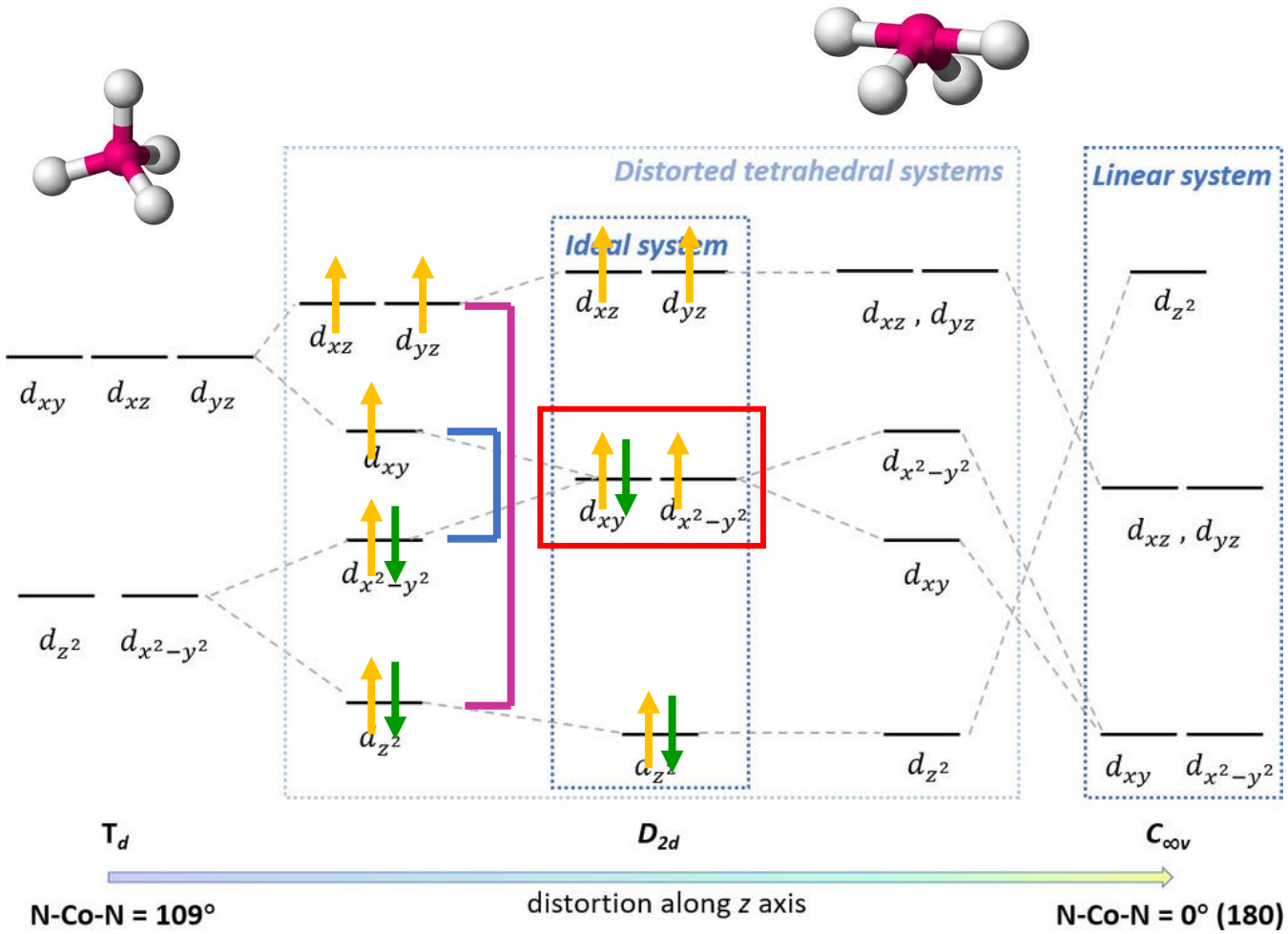

m_l	±2	± 1	0
	$d_{x^2-y^2}$	d_{xz}	d_{z^2}
	d_{xy}	d_{yz}	

Excitations with $\Delta|m_l| = 0$ contributes do D_{zz}

Excitations with $\Delta|m_l| = 1$ contributes to $(D_{xx}+D_{yy})/2$

The D_{ii} value depends **inversely** on excitation E.

If $|D_{zz}| > |(D_{xx}+D_{yy})/2|$ then D is negative

$d_{x^2-y^2} \rightarrow d_{xy}$ Large D_{zz}

$d_{z^2} \rightarrow d_{xy}/ d_{x^2-y^2}$ Small $(D_{xx}+D_{yy})/2$

LARGE NEGATIVE *D*

C. Legendre et al. *Eur. J. Inorg. Chem.*, **2021**, 8741

Tetra-coordinate Co(II)@surfaces

- Tetra-coordinate dinuclear Schiff base Co(II) complexes
- Ligand with acridine core – fluorescence
- Not SMM behavior but ferromagnetic ordering
- Deposited intact on highly ordered pyrolitic graphite by spin coating

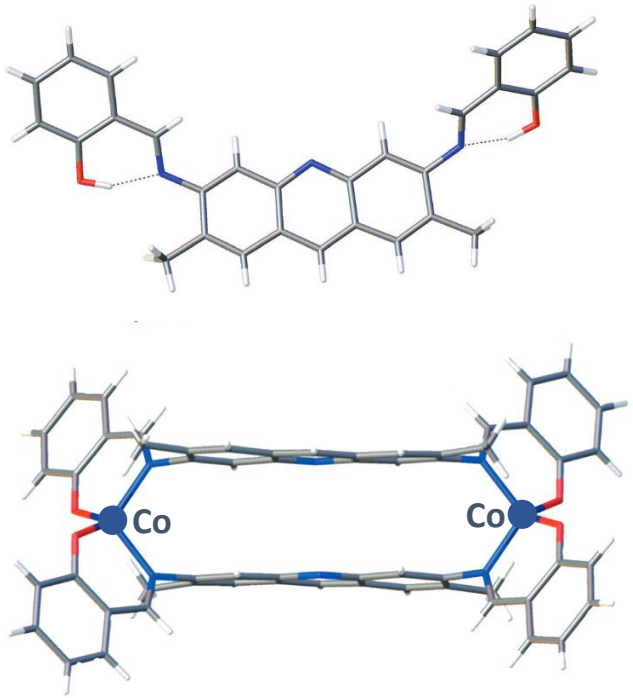

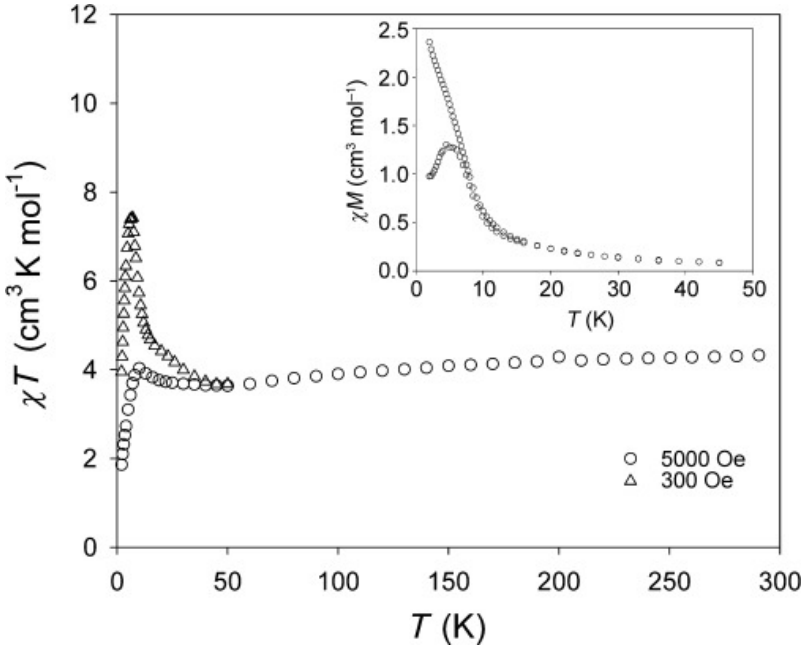

Not SMM but magnetic ordering

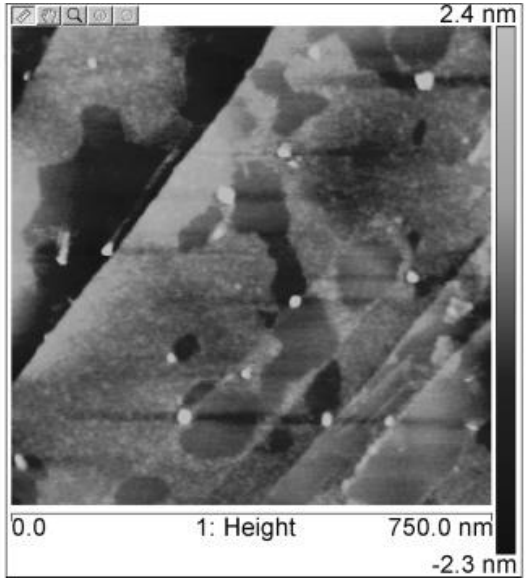

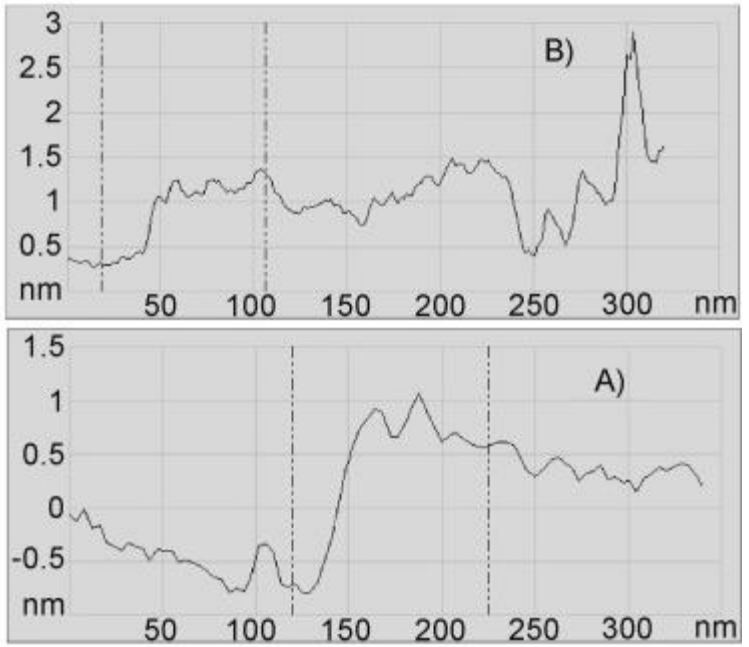

L. Spree et al. Adv. Funct. Materials, 2021, 31, 48, 105516

Tetra-coordinate Co(II)@surfaces

- Two tetra-coordinate complexes with ligands capable forming interactions with graphene
- Two kinds of deposition processes: thermal evaporation or wet techniques (drop-cast)

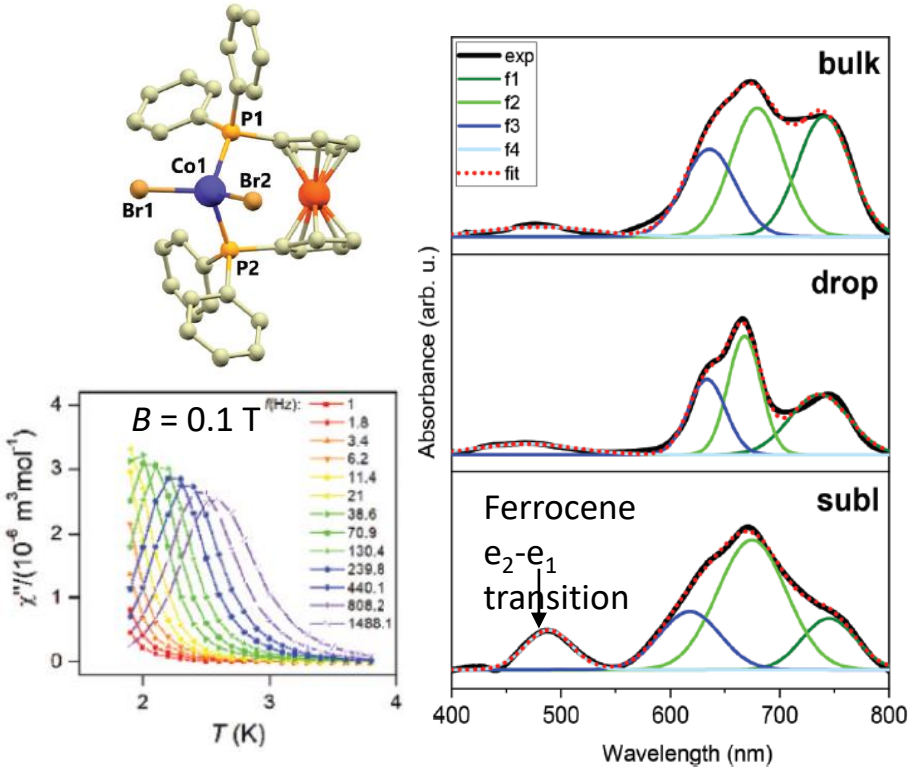

J. Hruby *et. al. Dalton Trans.* **2020**, 49, 11697

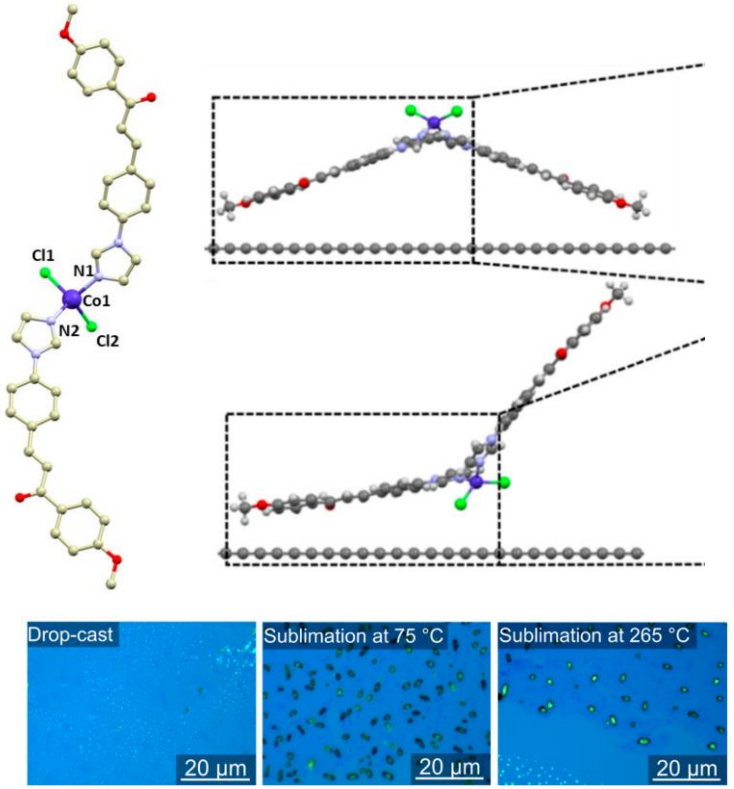

J. Hruby *et. al. Molecules.* **2020**, 25, 5021

Both deposits were very sensitive to moisture and molecules (partially) decomposed during sublimation.

Can we improve stability of the tetracoordinate molecules during an after deposition by using complexes with formally saturated (by semi-coordination) coordination sphere?

Motivation: Co(II) SIMs with bidentate Schiff base ligands

- Bidentate Schiff base ligands, N,O donor set
- Magnetic anisotropy is governed by deformation of tetrahedron (parameter of axial distortion ε_T)
- Zero-field SIMs (*D* = -20 to -50 cm^{-1})

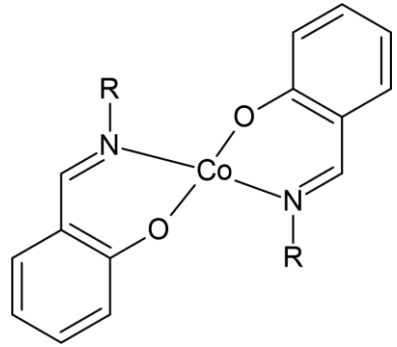

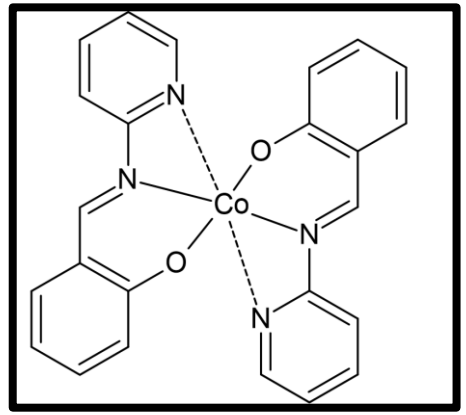

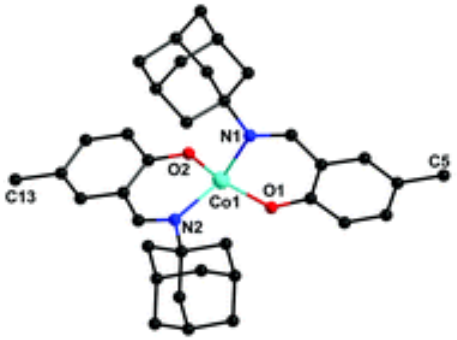

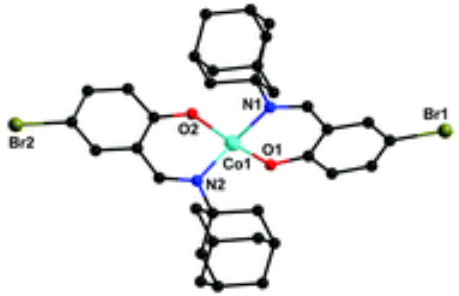

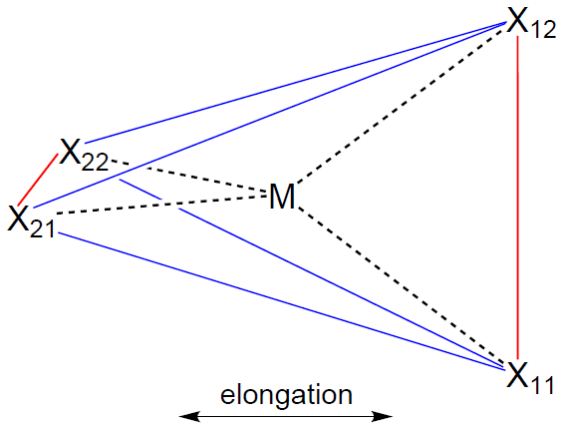

$$\epsilon_T = \frac{\alpha_o}{\alpha_a}$$

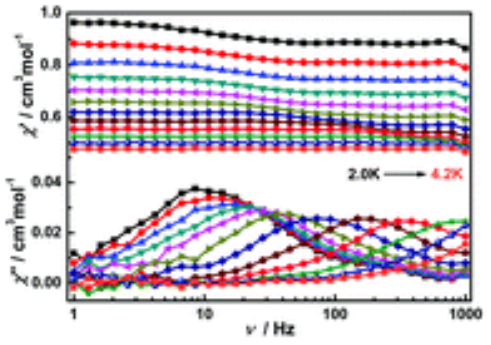

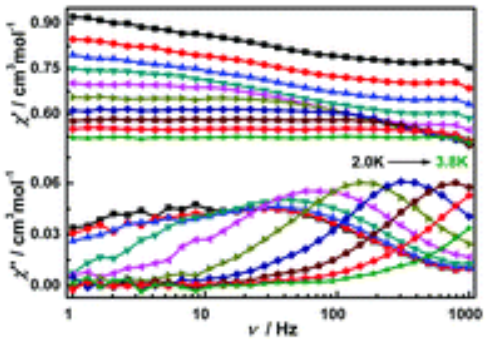

$$\alpha_o = \frac{1}{4}\sum_{i=1}^{2}\sum_{j=1}^{2}\angle X_{1i} M X_{2j}$$

$$\alpha_a = \frac{1}{2}\sum_{i=1}^{2}\angle X_{i1} M X_{i2}$$

bite angles

d(Co···N) > **2.6Å**

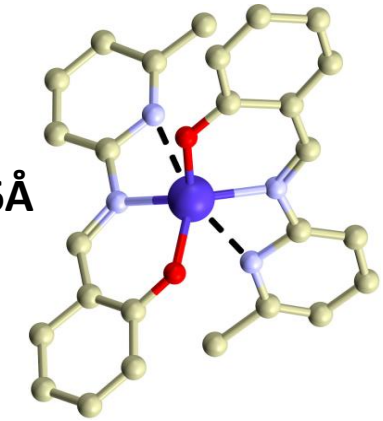

L. Xuet al., *Z. Strukt. Khimii*, **2006**, 47, 1003

Guo Peng et al. *Dalton Trans.*, **2020**, 49, 5798

S. Ziegenbalg et al. *Inorg. Chem.*, **2016**, 55, 8, 4047

Semi-coordination

- Noncovalent analog of the coordination bond introduced by Brown et al. in 1967, ‘intermediate type of bonding between coordination and nonbonding, very weakly coordinated’ [1]

- It usually implies the noncovalent nature of corresponding interactions with the major contribution derived from electrostatics and minor contributions from charge polarization and charge transfer [2]

- Simple initial criterion for the M···A pair: d(M ···A) < $\sum R_{vdW}$, but significantly longer than typical covalent bond (>> $\sum R_{cov}$)

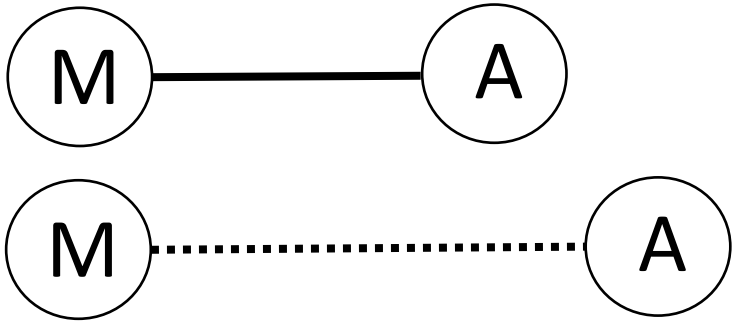

[1] I. V. Ananyev *et al*., *Acta Cryst. B76*, **2020**, 436–449
[2] Z.M. Efimenko *et al*., *Inorg. Chem*., **2020**, 59, 2316–2327.

Semi-coordination – QT-AIM

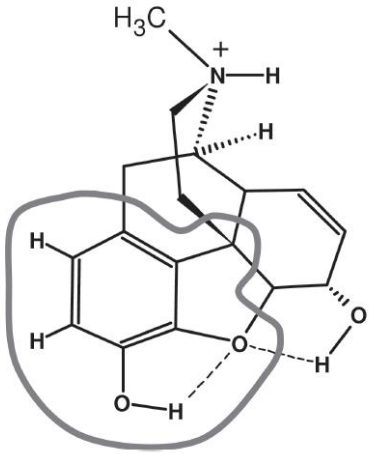

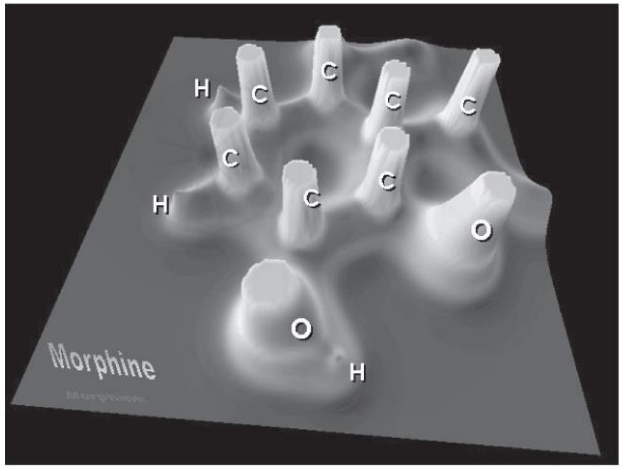

- The topology of electron density mainly shaped by the attractive forces of the nuclei, resulting in a significant peak at the location of each nucleus.
- A ‘‘critical point’’ (CP) in the electron density is a point in space at which the first derivatives of the density vanish

$$\nabla\rho = \mathbf{i}\frac{d\rho}{dx} + \mathbf{j}\frac{d\rho}{dy} + \mathbf{k}\frac{d\rho}{dz} \rightarrow \begin{cases} = \vec{\mathbf{0}} & \text{(At critical points and at } \infty\text{)} \\ \text{Generally} \neq \vec{\mathbf{0}} & \text{(At all other points)} \end{cases}$$

- To discriminate between local minimum and maximum – second derivative is calculated. Hessian matrix can be diagonalized and λ_1, λ_2 and λ_3 are curvatures of $\rho(\mathbf{r})$

$$\nabla^2\rho(\mathbf{r}) = \nabla\cdot\nabla\rho(\mathbf{r}) = \underbrace{\frac{\partial^2\rho(\mathbf{r})}{\partial x^2}}_{\lambda 1} + \underbrace{\frac{\partial^2\rho(\mathbf{r})}{\partial y^2}}_{\lambda 2} + \underbrace{\frac{\partial^2\rho(\mathbf{r})}{\partial z^2}}_{\lambda 3}$$

$$\mathbf{\Lambda} = \begin{pmatrix} \frac{\partial^2\rho}{\partial x'^2} & 0 & 0 \\ 0 & \frac{\partial^2\rho}{\partial y'^2} & 0 \\ 0 & 0 & \frac{\partial^2\rho}{\partial z'^2} \end{pmatrix}_{\mathbf{r}'=\mathbf{r}_c} = \begin{pmatrix} \lambda_1 & 0 & 0 \\ 0 & \lambda_2 & 0 \\ 0 & 0 & \lambda_3 \end{pmatrix}$$

R. F. W. Bader *Atoms in Molecules A Quantum Theory* **1994**, Oxford Uni Press

Semi-coordination – QT-AIM

- Critical points are classified according to their rank (ω) and signature (σ), whereas $\omega = 3$ and are symbolized by (3, σ). The rank is the sum of non-zero curvatures of ρ at the critical point ($\lambda_1 + \lambda_2 + \lambda_3$).

Bond critical point BCP!

- $(3, -3)$ Three negative curvatures: ρ is a local maximum.
- $(3, -1)$ Two negative curvatures: ρ is a maximum in the plane defined by the corresponding eigenvectors but is a minimum along the third axis which is perpendicular to this plane.
- $(3, +1)$ Two positive curvatures: ρ is a minimum in the plane defined by the corresponding eigenvectors and a maximum along the third axis which is perpendicular to this plane.
- $(3, +3)$ Three curvatures are positive: ρ is a local minimum.

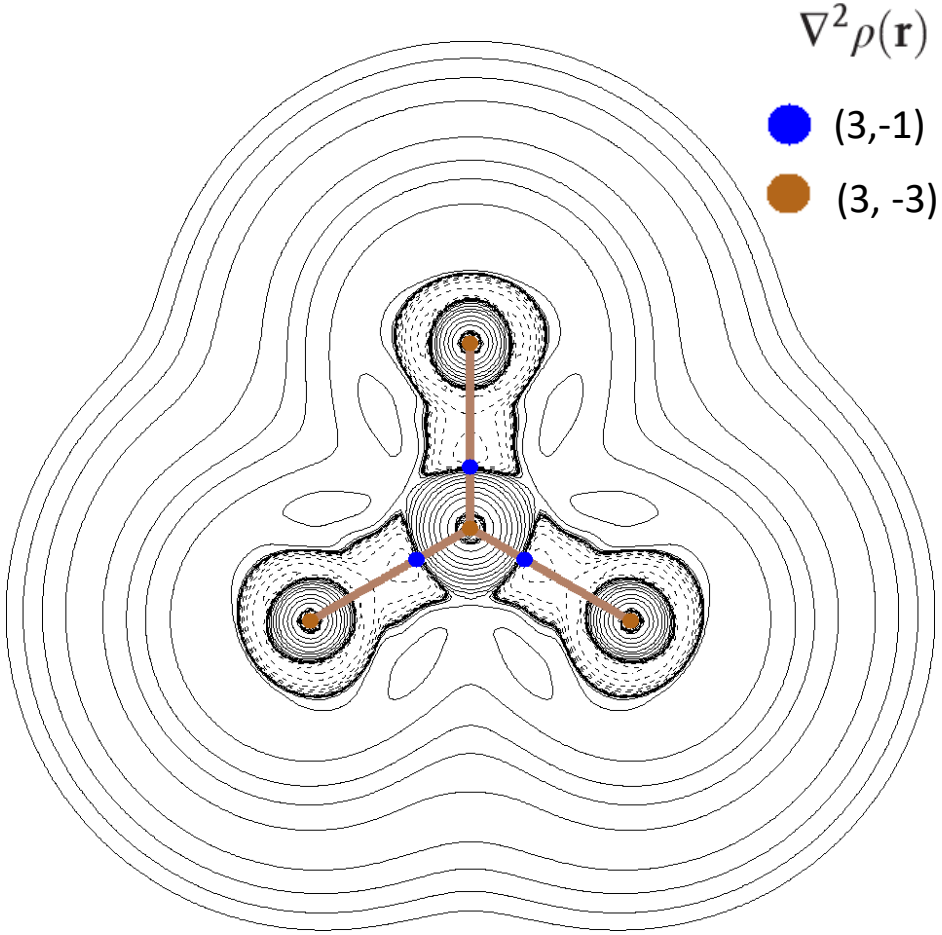

Semi-coordination – QT-AIM

- At BCP we calculate parameters determining topology and energetic properties of $\rho(\mathbf{r})$:
- $G(\mathbf{r})$ kinetic energy density, $V(\mathbf{r})$ potential energy density – virial, $H(\mathbf{r})$ full energy density
- At BCP $H(\mathbf{r})$ is negative for interactions with significant sharing of electrons, positive for non-covalent int.
- At BCP $|V(\mathbf{r})|/G(\mathbf{r}) < 1$, if larger than 1, increasing covalency
- Strength of interaction can be estimated from virial $-V(\mathbf{r})/2$

$$\left(\frac{\hbar^2}{4m}\right)\nabla^2\rho(\mathbf{r}) = 2G(\mathbf{r}) + \mathscr{V}(\mathbf{r}) \qquad H(\mathbf{r}) = G(\mathbf{r}) + V(\mathbf{r}) \qquad E_{int} = -V(\mathbf{r})/2$$

- In line with this the definition of semi-coordination at the (3, −1) BCP is:

(1) **attractive** non-covalent interaction: $\nabla^2\rho(\mathbf{r}) > 0$ and $H(\mathbf{r}) > 0$)

($2|V(\mathbf{r})|/G(\mathbf{r}) < 1.0$ for non-covalent interactions

[1] I. V. Ananyev *et al*., *Acta Cryst. B76*, **2020**, 436–449
[2] Z.M. Efimenko *et al*., *Inorg. Chem*., **2020**, 59, 2316–2327.
[3] E. Espinosa *et al*., *J. Chem. Phys*. **2002**, 117, 5529

Semi-coordination and magnetism

- The Single-ion Magnets (SIMs) often contain M–A bonds which fulfil initial criterion, *e.g*. complexes with macrocyclic ligands. How are the ligand field and magnetic anisotropy affected?

- Semi-coordination can affect magnetic properties. Mediation of ferromagnetic exchange interaction in $NaCu(CO_3)_2$ or antiferromagnetic exchange interaction in the Cu(II) complex.

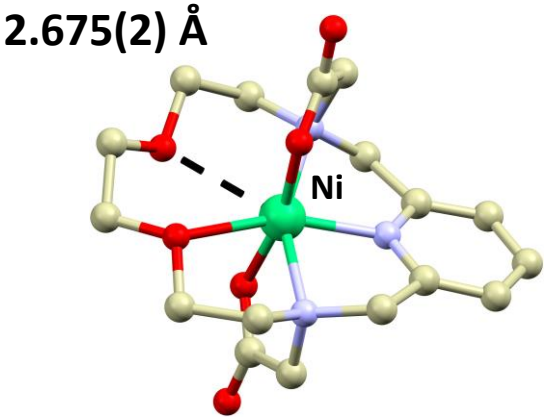

B. Drahos *et al*. *EJIC*., **2018,** 4286.

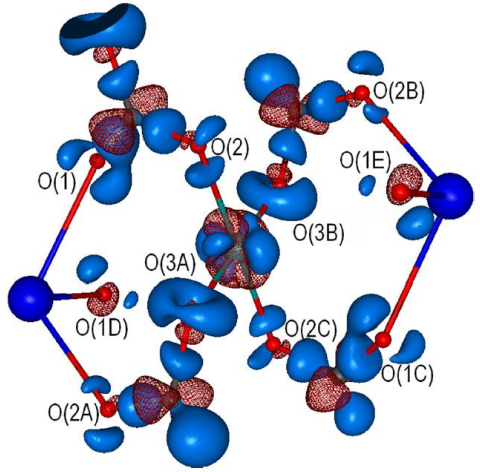

Y.V. Nelyubina *et al*. *Inorg. Chem.* **2013**, 52, 14355.

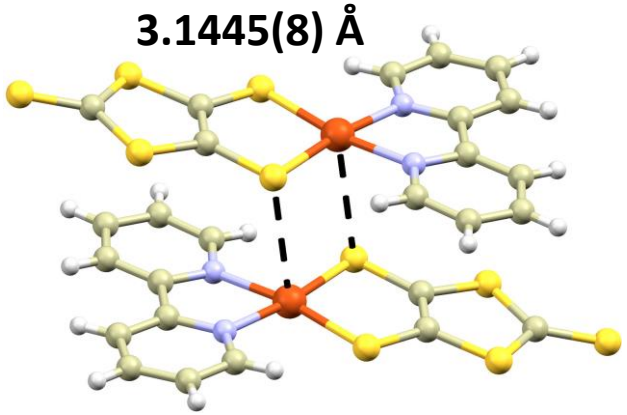

V.A. Starodub *et al*. *J. Phys. Chem. Sol.* **2013**, 73, 2, 350.

Co(II) SMMs & semi-coordination

D. Jayatilaka and M.A. Spackman, *CrystalExplorer package*

- $[Co(dpt)(NCS)_2]$, dpt = dipropylenetriamine

  $Co(NCS)_2 + dpt = [Co(dpt)(NCS)_2]$

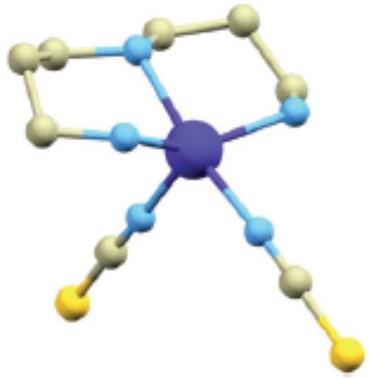

Pentacoordinate
$\tau = 0.46$

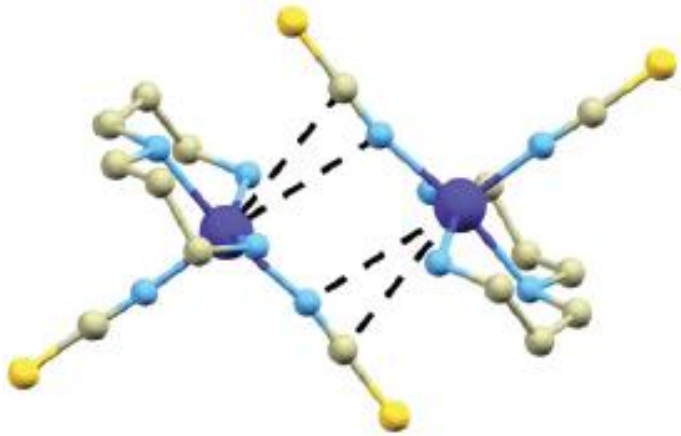

d(Co···N) = 3.541(2) Å
d(Co···C) = 3.652(2) Å
d(Co···Cg) = 3.550 Å

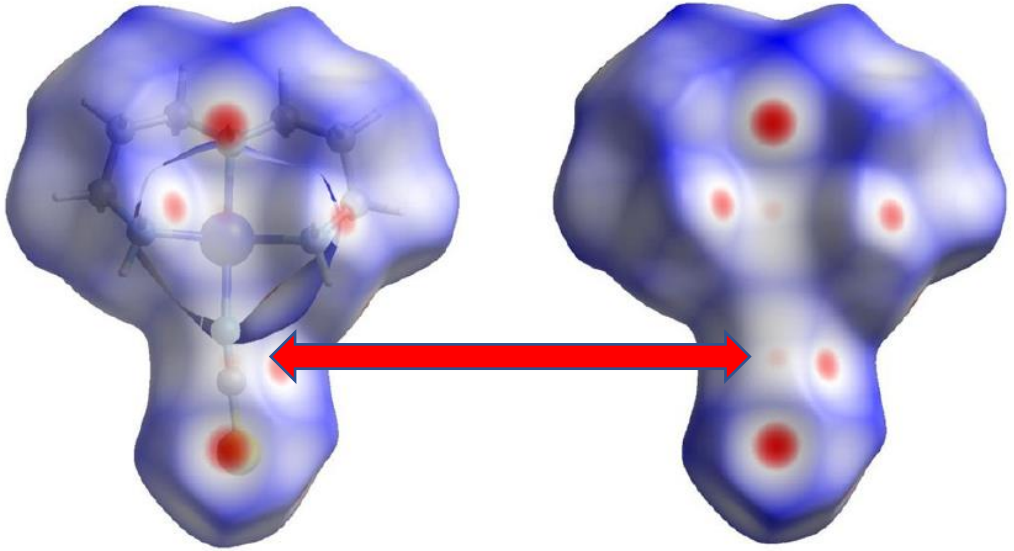

Hirschfeld surface
(d_{norm})

I. Nemec et al. *Dalton Trans*., **2016**, (31), 12479

Co(II) SMMs & semi-coordination

- $[Co(dpt)(NCS)_2]$, dpt = dipropylenetriamine

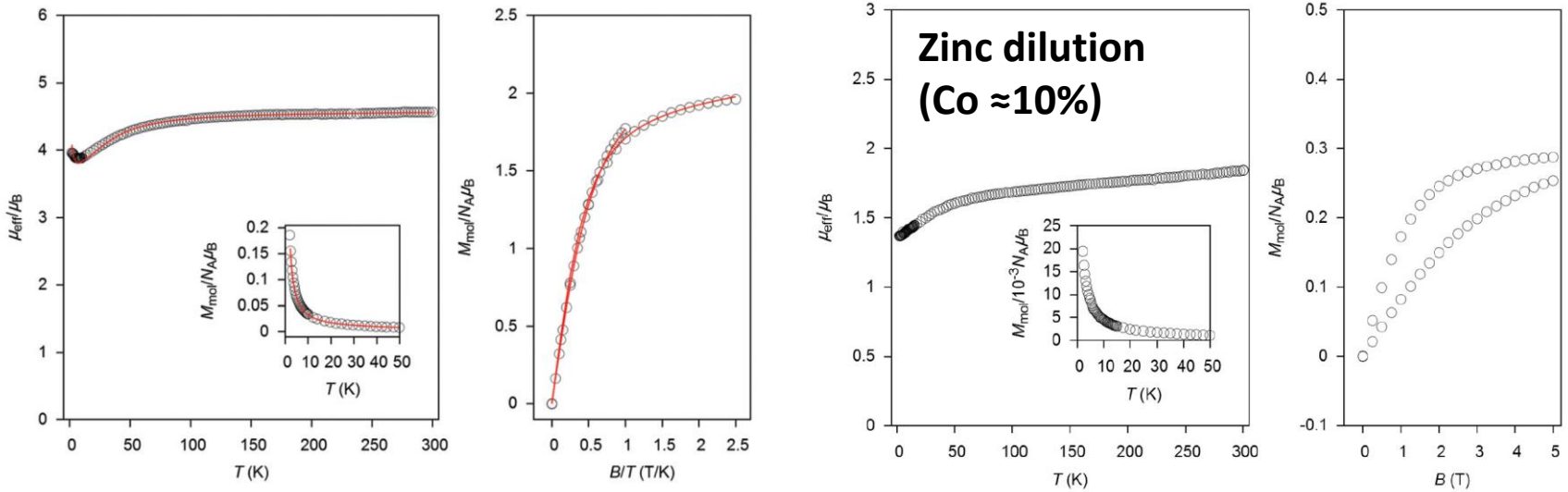

AC magnetism

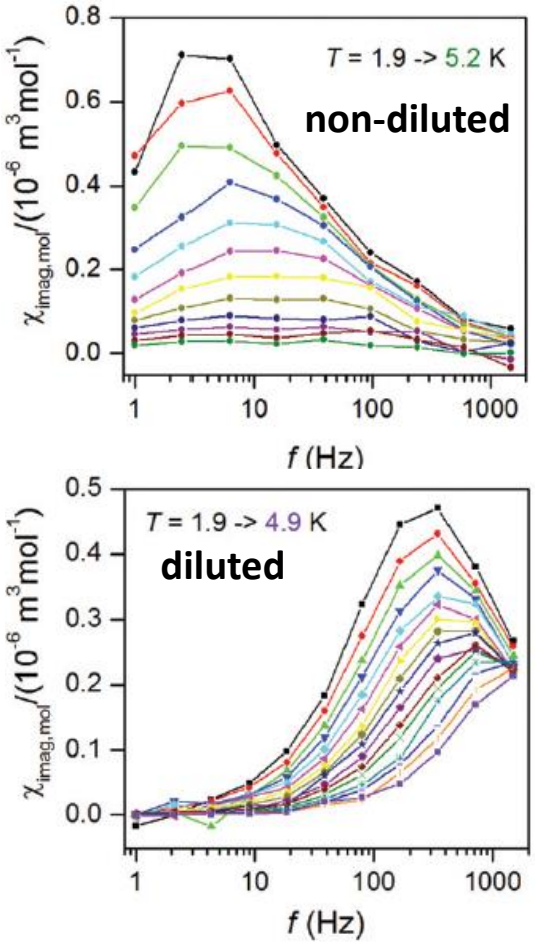

$$\hat{H} = -J(\vec{S}_1 \cdot \vec{S}_2) + \sum_{i=1}^{2} D_i(\hat{S}_{z,i}^2 - \hat{S}_i^2/3) + E_i(\hat{S}_{x,i}^2 - \hat{S}_y^2) + \mu_B B g_i \hat{S}_{a,i}$$

J = +0.25 cm^{-1}, $|D|$ = 36 cm^{-1},
E/D = 0.22 (D<0), 0.33 (D>0)

CASSCF/NEVPT2:
D = +34.0 cm^{-1}, E/D = 0.22

I. Nemec et al. *Dalton Trans.*, **2016**, (31), 12479

Co(II) SMMs & semi-coordination

- [Co(dpt)(NCS)$_2$], theoretical investigations

BS-DFT calculations
B3LYP/ZORA/-def2-TZVP(-f)

J = +0.22 cm^{-1}

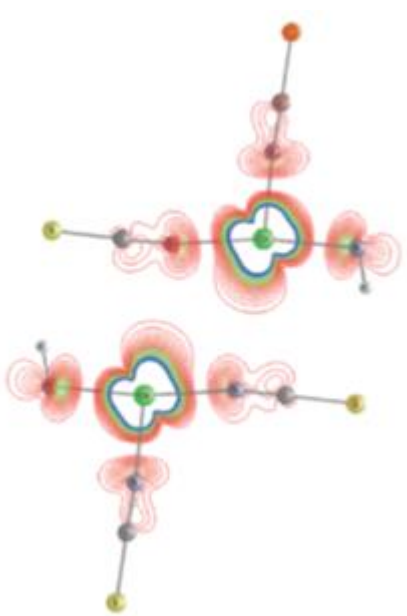

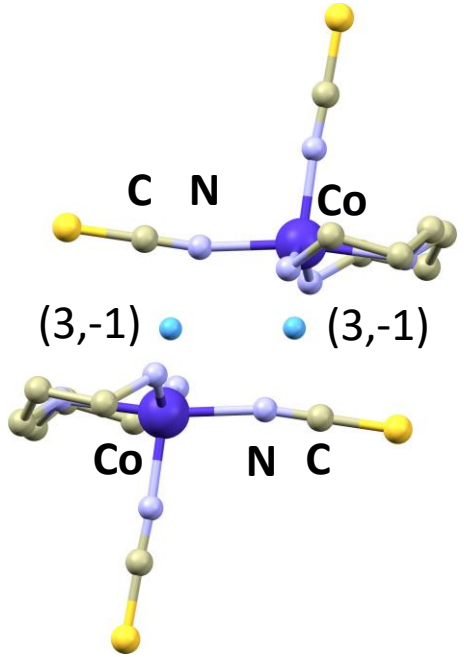

Non-covalent exchange pathway

L. Havlicek et al. *Polyhedron*., **2022**, (223), 115962

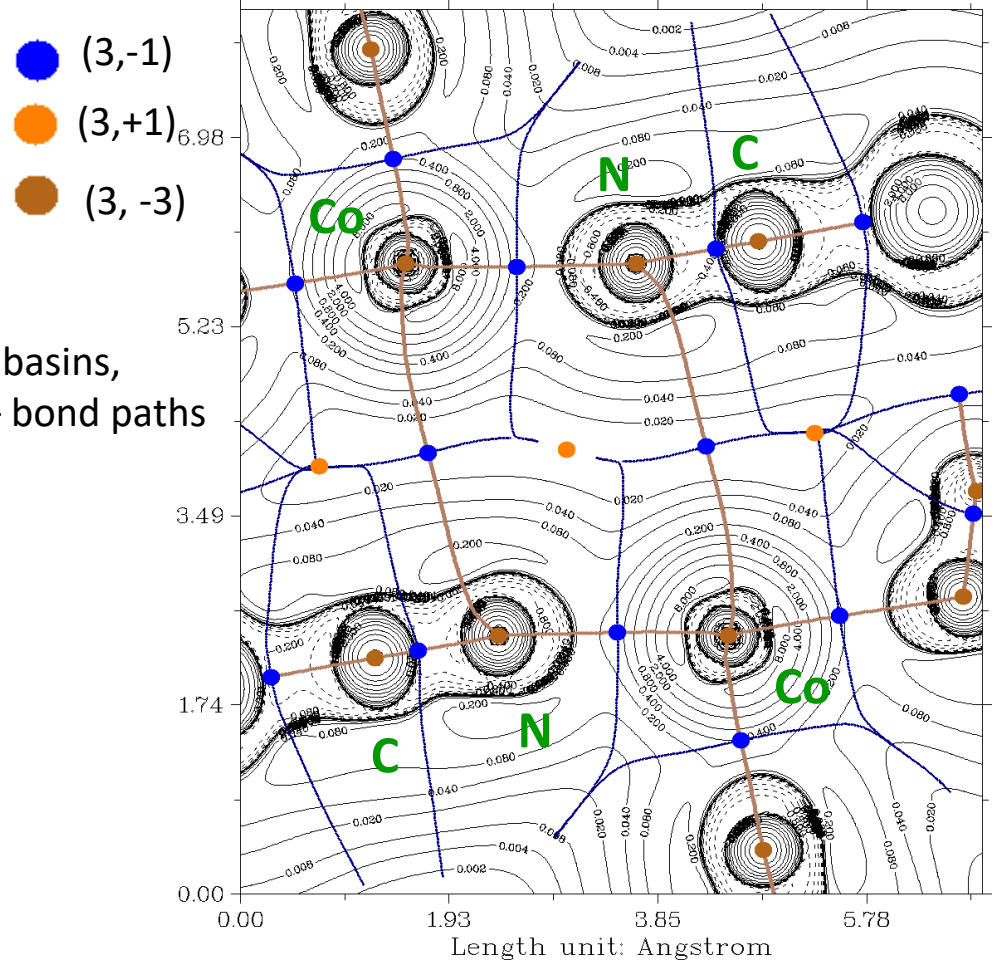

blue lines – basins,
brown lin. – bond paths

BCPs for Co···N:
type (3,-1)

$E_{int} = |V(r)|/2$ = 1.6 kcal/mol

$\nabla^2\rho(r)$ = 0.0126267
$H(r)$/a.u. = 0.000321
$V(r)$/a.u. = -0.002513
$G(r)$ /a.u. = 0.002835

$\nabla^2\rho(r) > 0$
$H(r) > 0$
$|V(r)|/G(r) = 0.886 < 1$
non-covalent character

Co(II) SMMs with bidentate Schiff base ligands

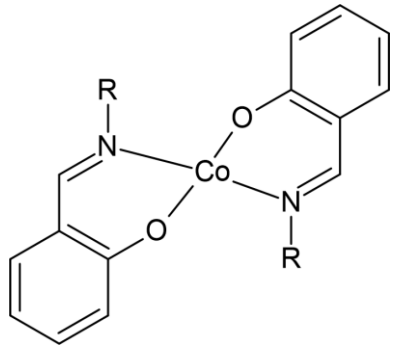

(i) Structural/QT-AIM investigations

(ii) Magnetism

(iii) Depositions by thermal evaporation

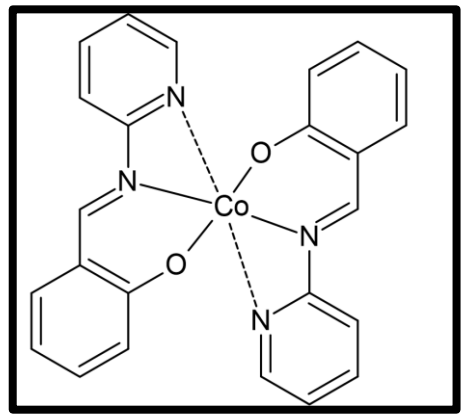

d(Co···N) > **2.6Å**

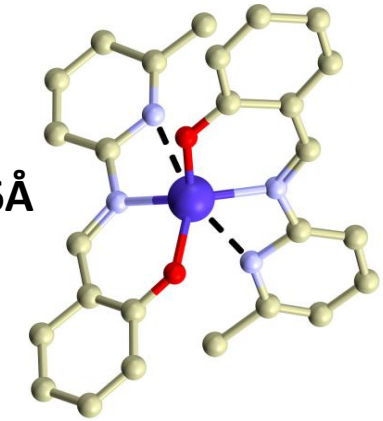

L.Xuet al., *Z. Strukt. Khimii*, **2006**, 47, 1003

Synthesis

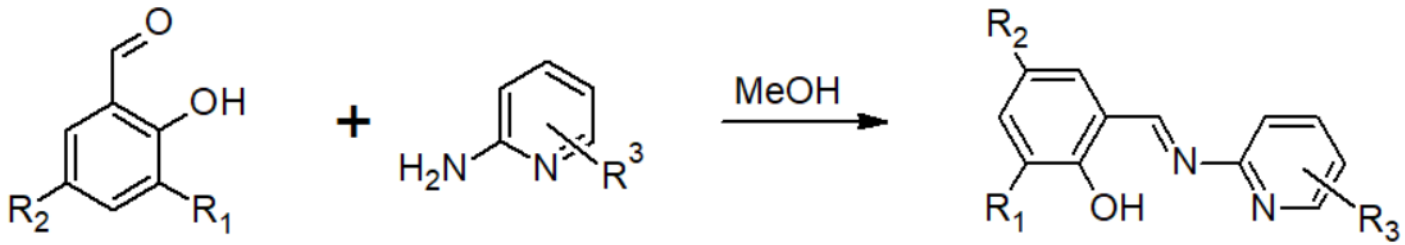

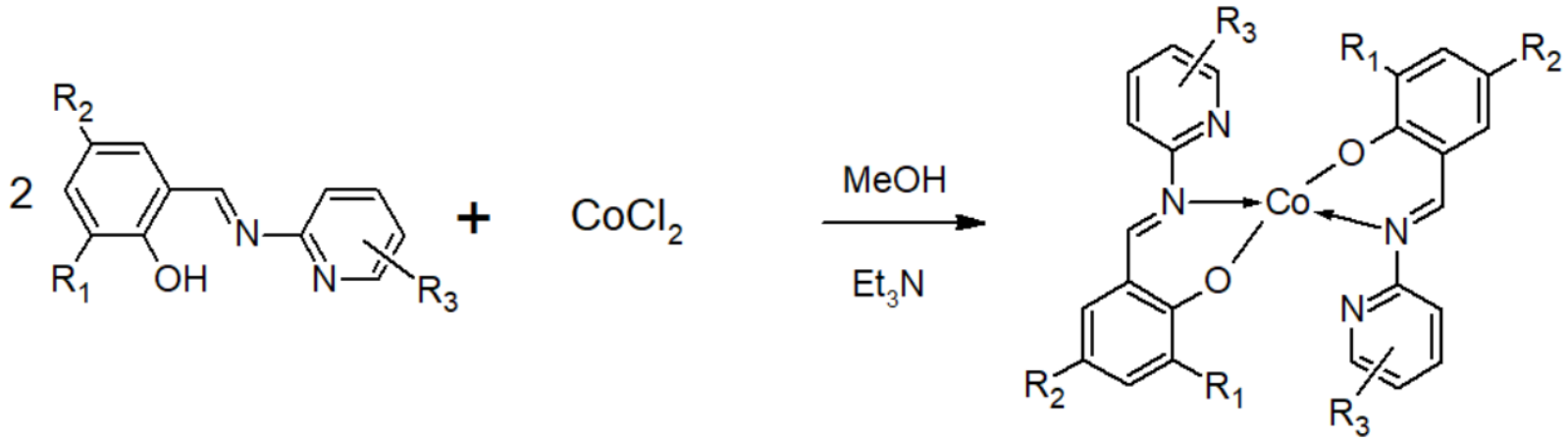

Petr Přecechtěl & Ondřej F. Fellner
Palacky Uni Olomouc

$R_1 = R_2$ = -H, -X, -OMe, -NO_2

R_3 = -H, -X, -CH_3, -CH_2CH_3, -CF_3

Different reaction conditions (stoichiometric ratios, pH, reaction times…) → polynuclear complexes

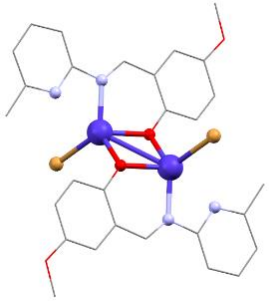

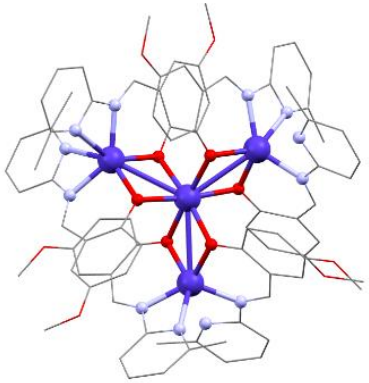

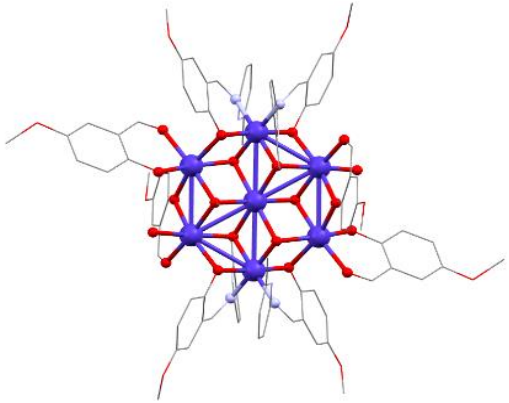

Crystal structure

c.n. 4+2

c.n. 4+1

c.n. 4

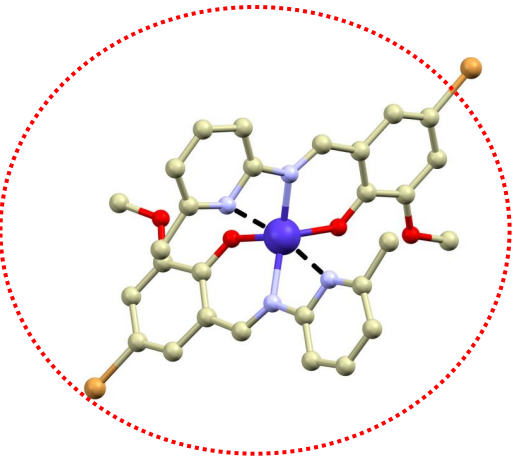

d(Co···N) = **2.499(2), 2.565(2) Å**

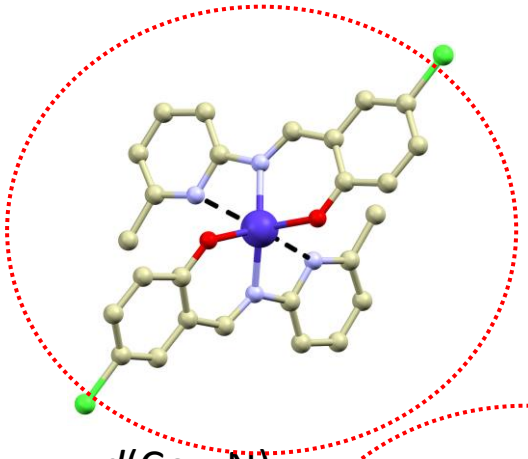

d(Co···N) = **2.614(2) Å**

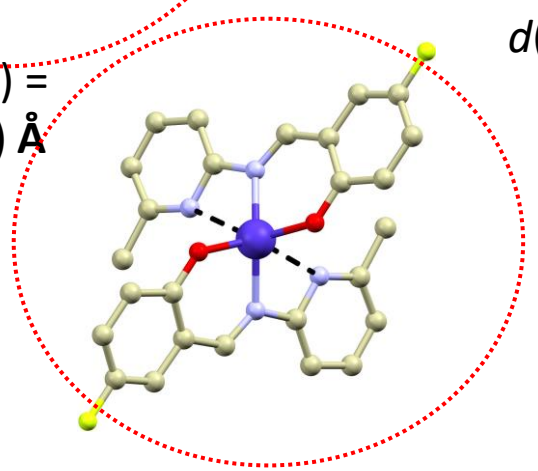

d(Co···N) = **2.659(2) Å**

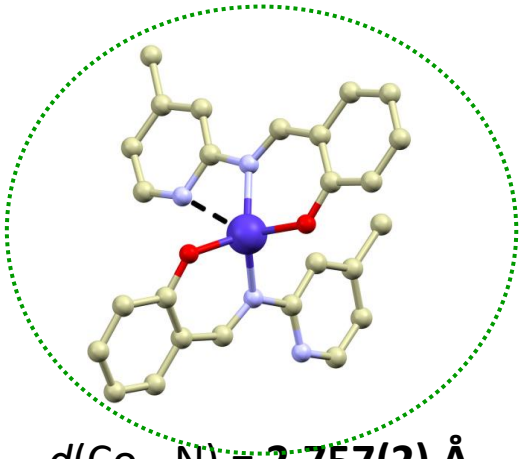

d(Co···N) = **2.757(2) Å**

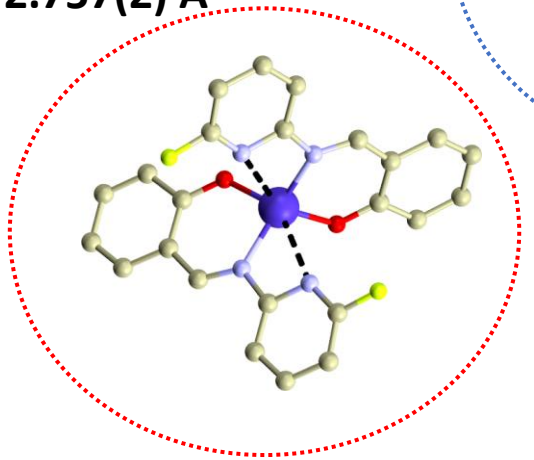

d(Co···N) = **2.801(4) Å**

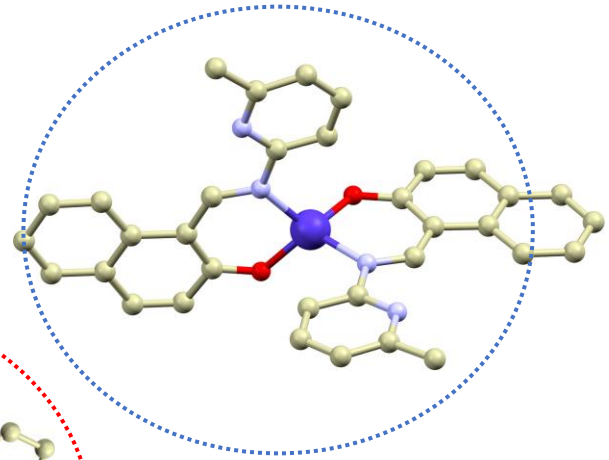

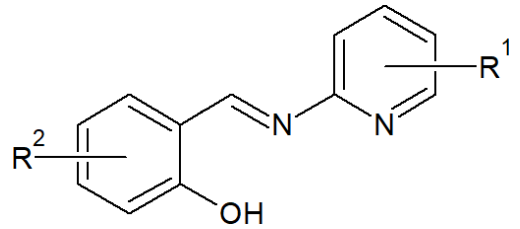

Shape of coordination polyhedron

S. Alvarez *Chem. Rev.* **2015**, 115, 24, 13447–13483

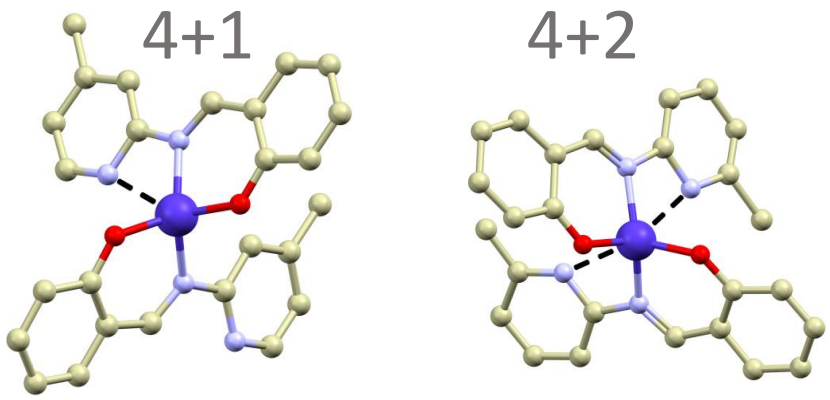

$$\epsilon_T = \frac{\alpha_o}{\alpha_a}$$

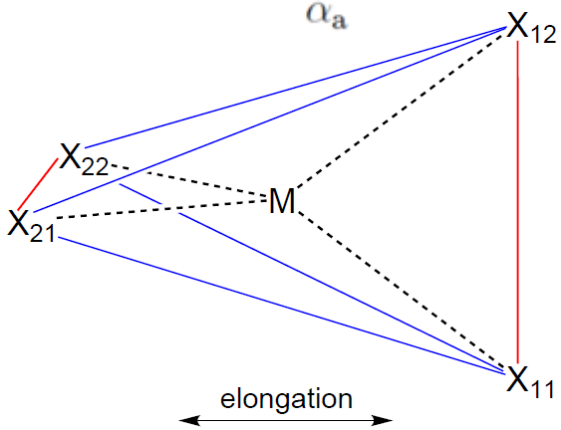

Axial elongation

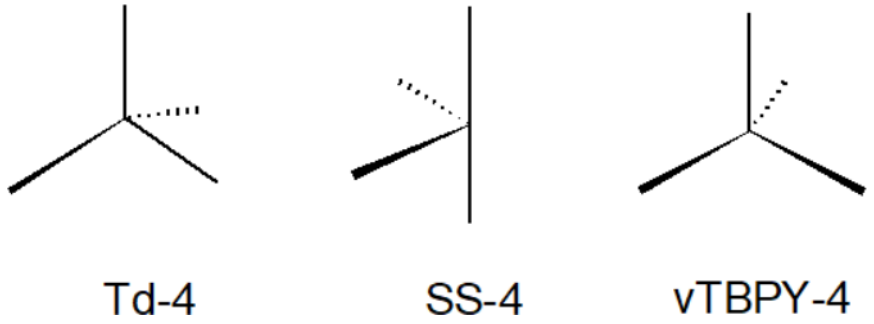

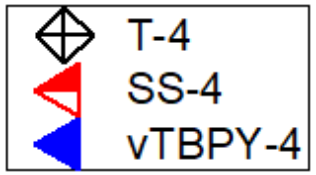

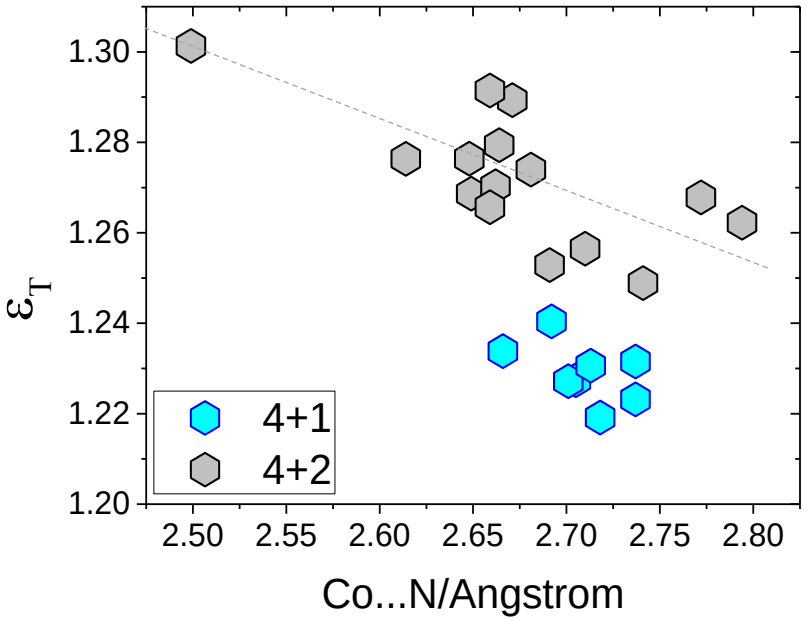

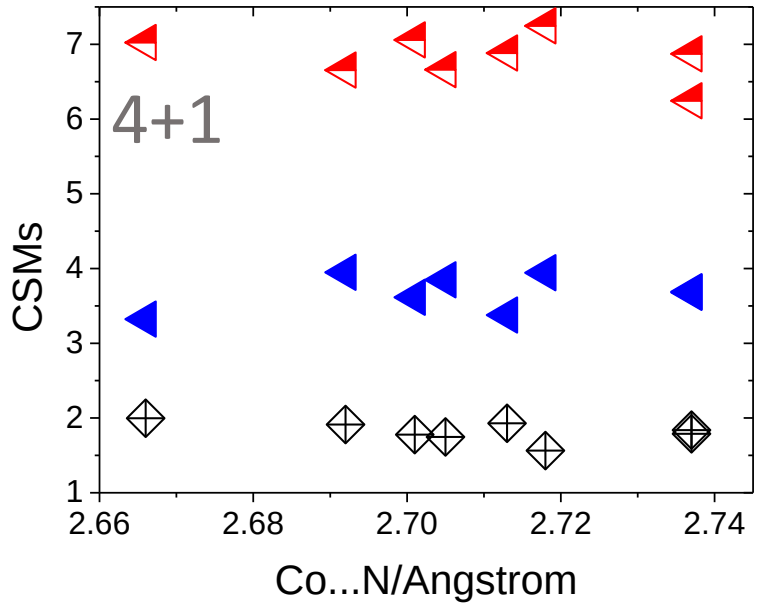

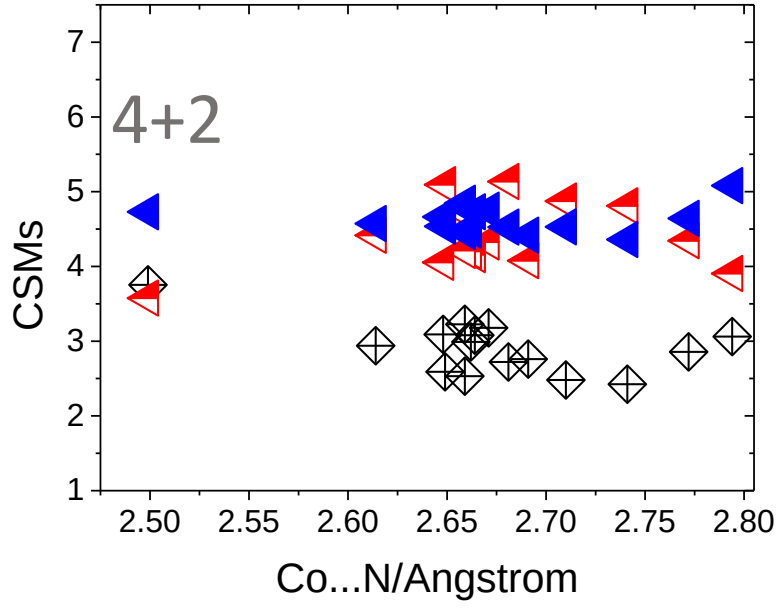

shorter Co···N distance ≈ larger axial distortion

4+2 geometry exhibits larger distortions

QT-AIM

$\nabla^2\rho(\mathbf{r})$ B3LYP (def2-TZVP)

(3,-1)
(3,+1)
(3, -3)

[Co(3MeO-5Br-pymep)$_2$]

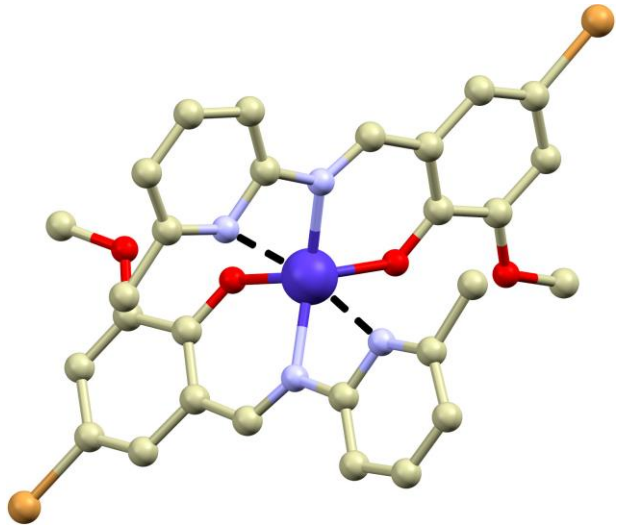

d(Co···N) = 2.499(2), 2.565(2) Å

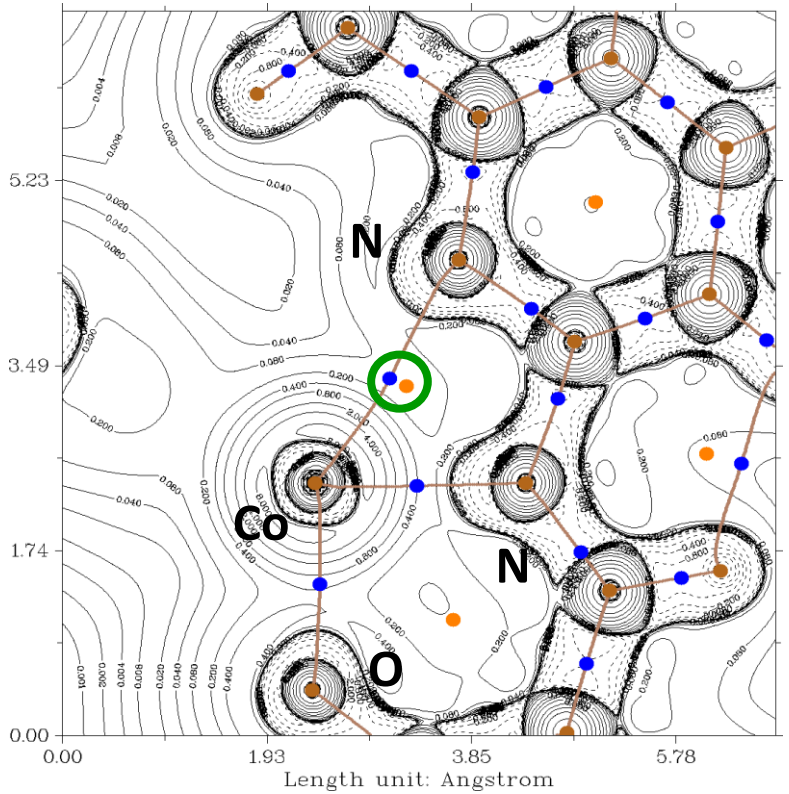

***d*(Co···N) = 2.499(2) Å**

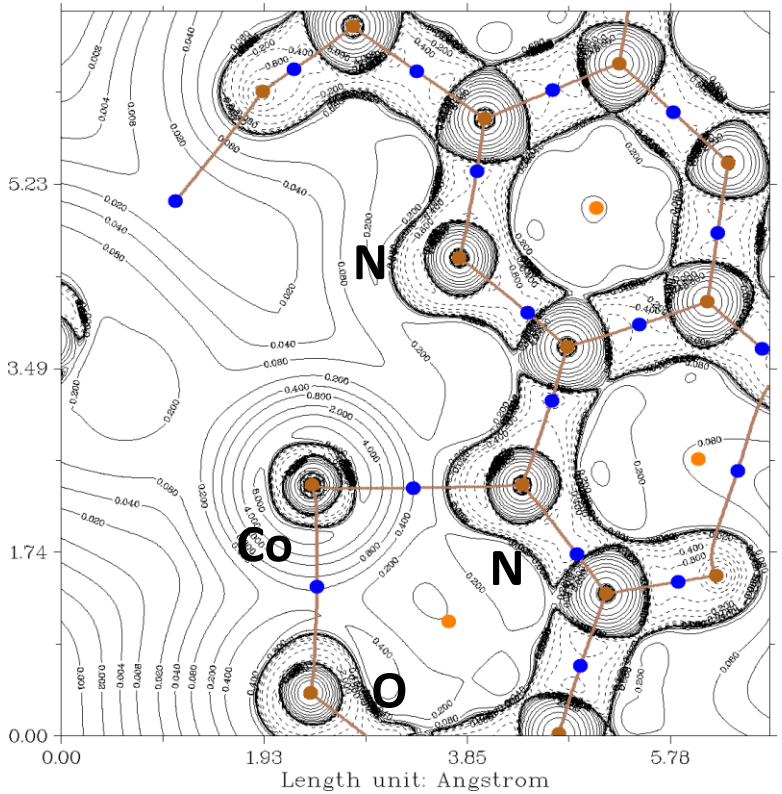

***d*(Co···N) = 2.565 (2) Å**

BCPs for Co···N:
type (3,-1)

$\boldsymbol{V}(\mathbf{r})$/a.u. = -0.02878
$\boldsymbol{H}(\mathbf{r})$/a.u. = -0.0007
$\boldsymbol{G}(\mathbf{r})$ /a.u. = 0.02807
$\nabla^2\rho(\mathbf{r})$ = 0.1095

$\nabla^2\rho(\mathbf{r}) > 0$, $\boldsymbol{H}(\mathbf{r}) < 0$
weakly covalent character

$|\boldsymbol{V}(\mathbf{r})|/\boldsymbol{G}(\mathbf{r}) = 1.03 > 1$
weak covalent character

$E_{int} = |\boldsymbol{V}(\mathbf{r})|/2 =$ 9.0 kcal/mol

other Co-N/O bonds: 42-55 kcal/mol

QT-AIM

A. D. Becke and K. E. Edgecombe, *J. Chem. Phys*. **1990**, 92, 5397

E.R. Johnson et al. *J. Am. Chem. Soc*. **2010**, 132, 18

$[Co(pymep)_2]$

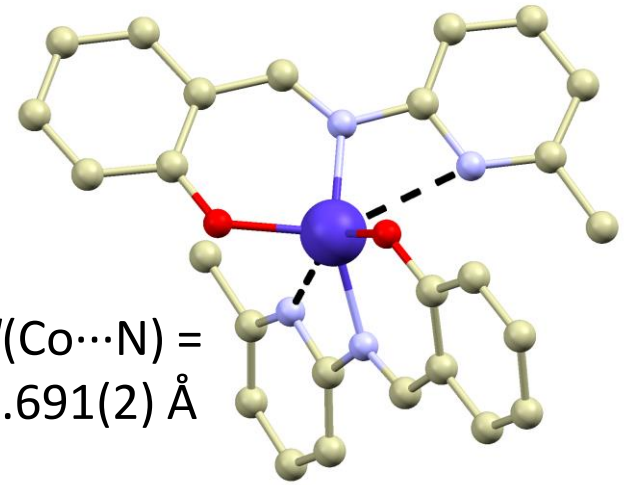

d(Co···N) = 2.691(2) Å

$\nabla^2\rho(\mathbf{r})$

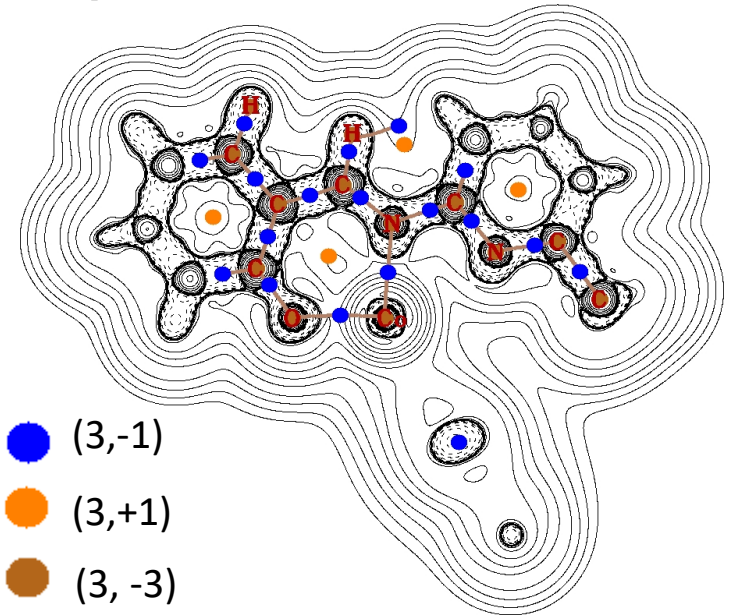

Electron localization function

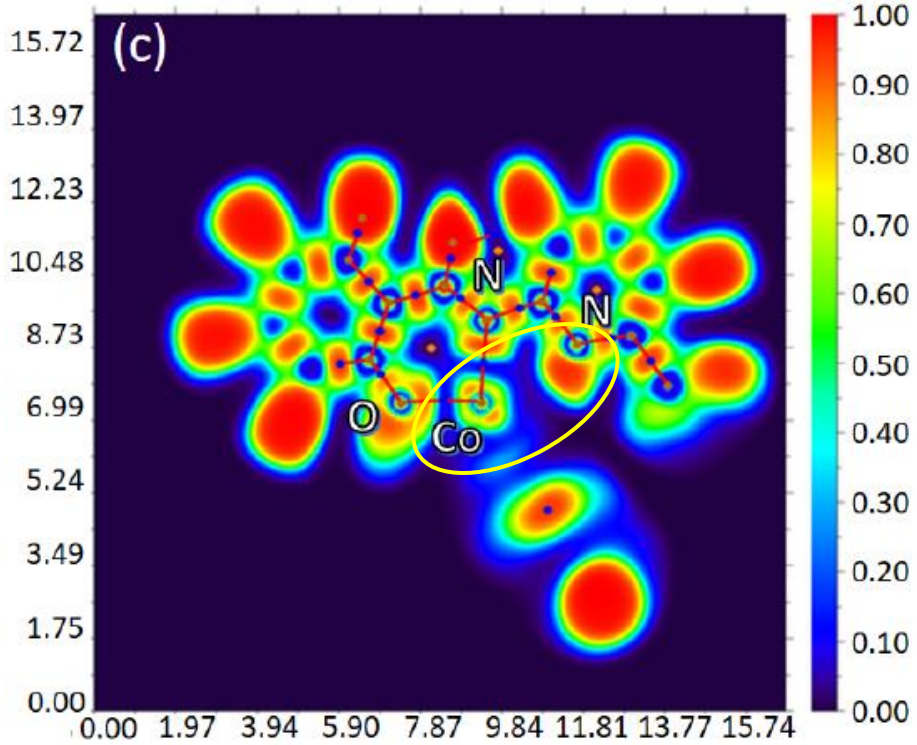

Non-covalent interaction index

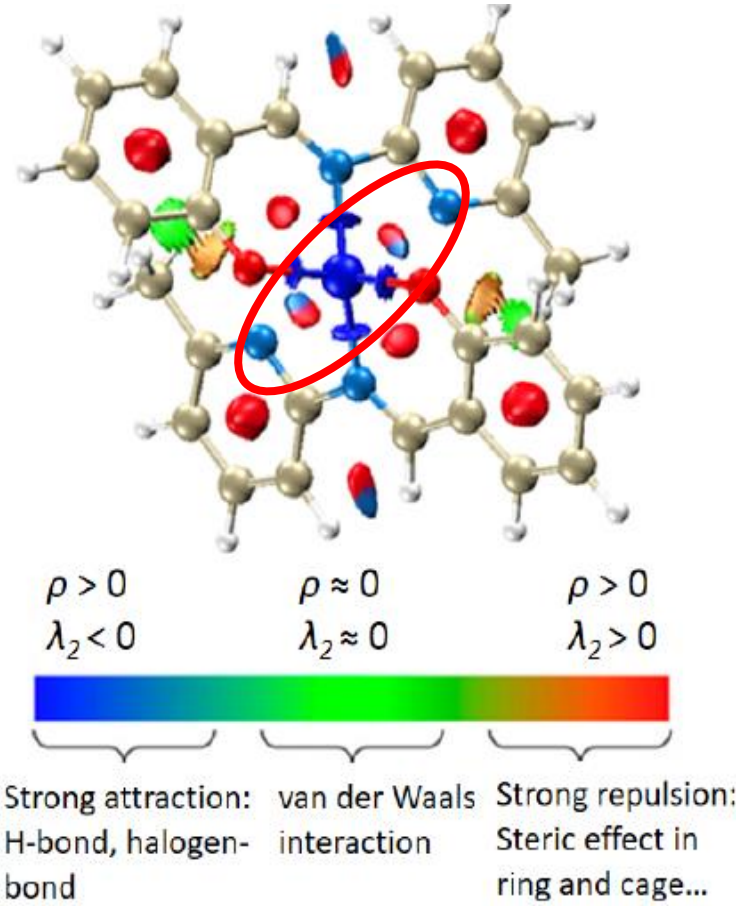

No BCP but interaction is attractive and very likely with dominant electrostatic character

J. Navarro et al, *PCCP*. **2023**, 25, 29516

Magnetic properties

Magnetism – DC data

$$\hat{H} = -J\left(\hat{S}_1 \cdot \hat{S}_2\right) + D\left(\hat{S}_z^2 - \frac{S^2}{3}\right) + E\left(\hat{S}_x^2 - \hat{S}_y^2\right) + \mu_B B g \hat{S}_a$$

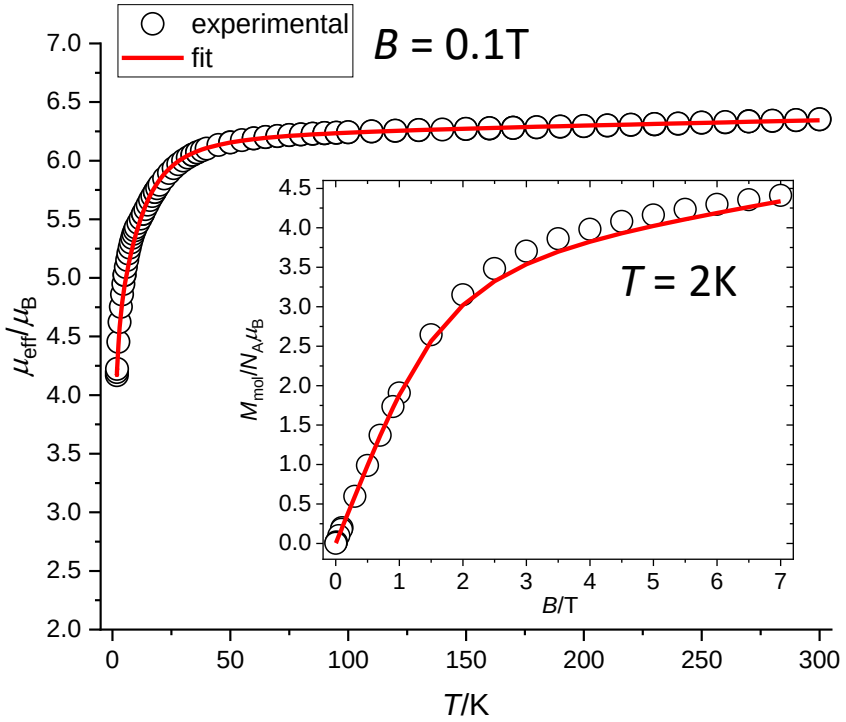

BS-DFT

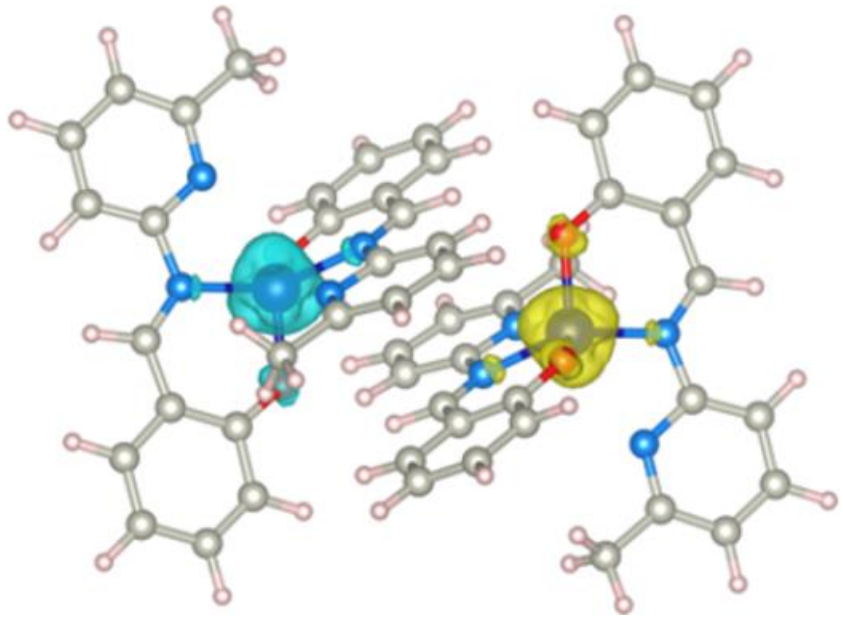

g_{iso} = 2.272, D = -15.3 cm^{-1}, E/D = 0.012, J = –0.27 cm^{-1}

J = –0.25 cm^{-1}
B3LYP/ZORA/-def2-TZVP(-f)

J. Navarro et al, *PCCP*. **2023**, 25, 29516

Magnetic properties

Magnetism – HF-EPR

no zero-field absorption observed

$D < -20\text{cm}^{-1}$, $E/D = 0.122$, $J = -0.3\ \text{cm}^{-1}$

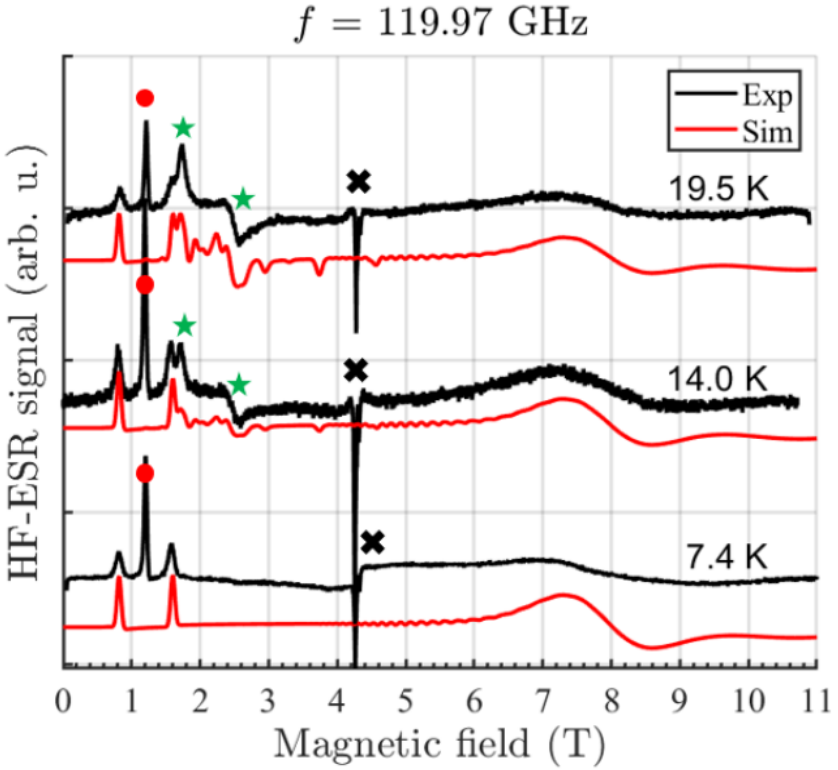

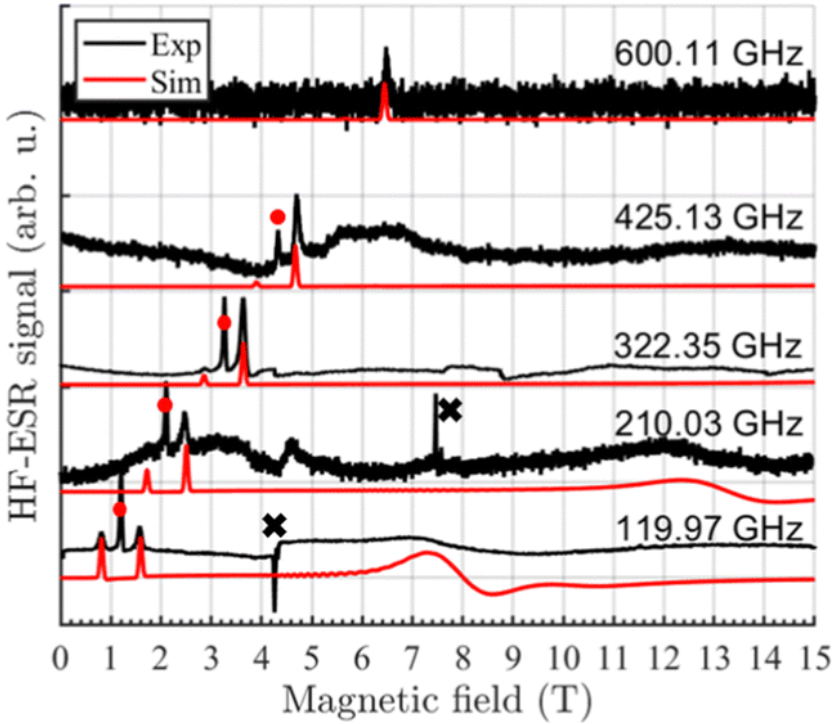

Vinicus T. Santana
CEITEC Brno

J. Navarro et al, *PCCP*. **2023**, 25, 29516

CASSCF/NEVPT2 calculations
AILFT

The lowest LF terms are all quartets

D = -24.2 cm^{-1}, E/D = 0.084
(magnetometry: D = -15.3 cm^{-1}, E/D = 0.012
HFEPR: D < -20cm^{-1}, E/D = 0.122)

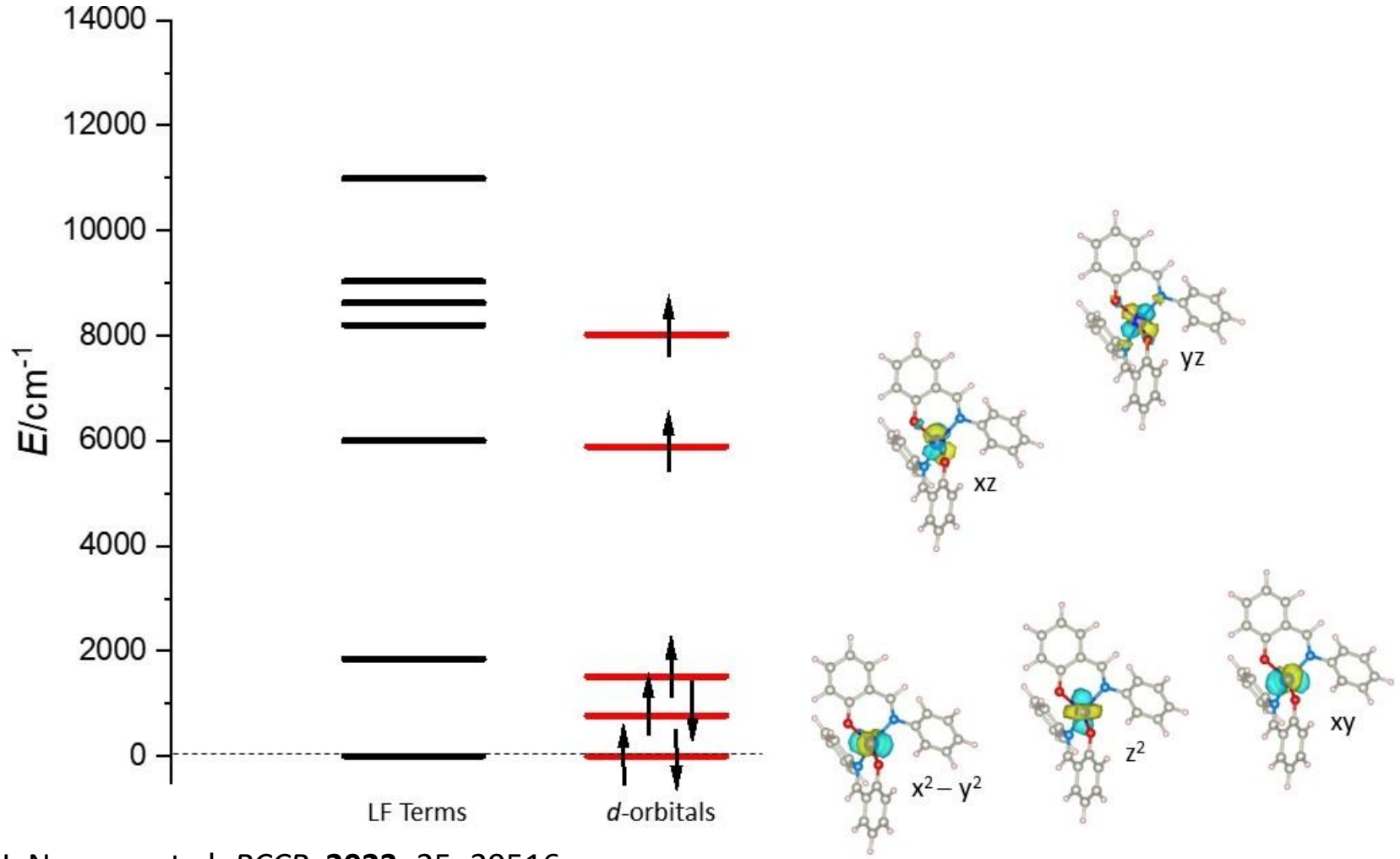

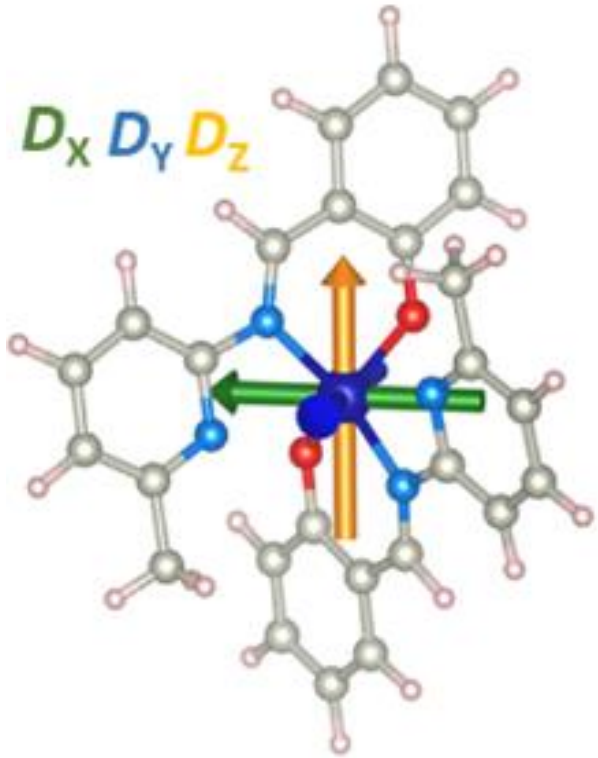

J. Navarro et al, *PCCP*. **2023**, 25, 29516

CASSCF/NEVPT2 calculations

crystal structure coordinates

d(Co···N) = 2.6951(9) Å

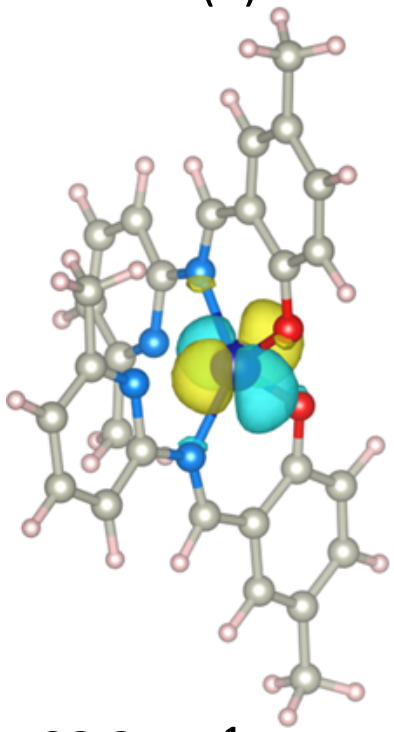

***D* = -28.3 cm^{-1}**

***E*/*D* = 0.11**

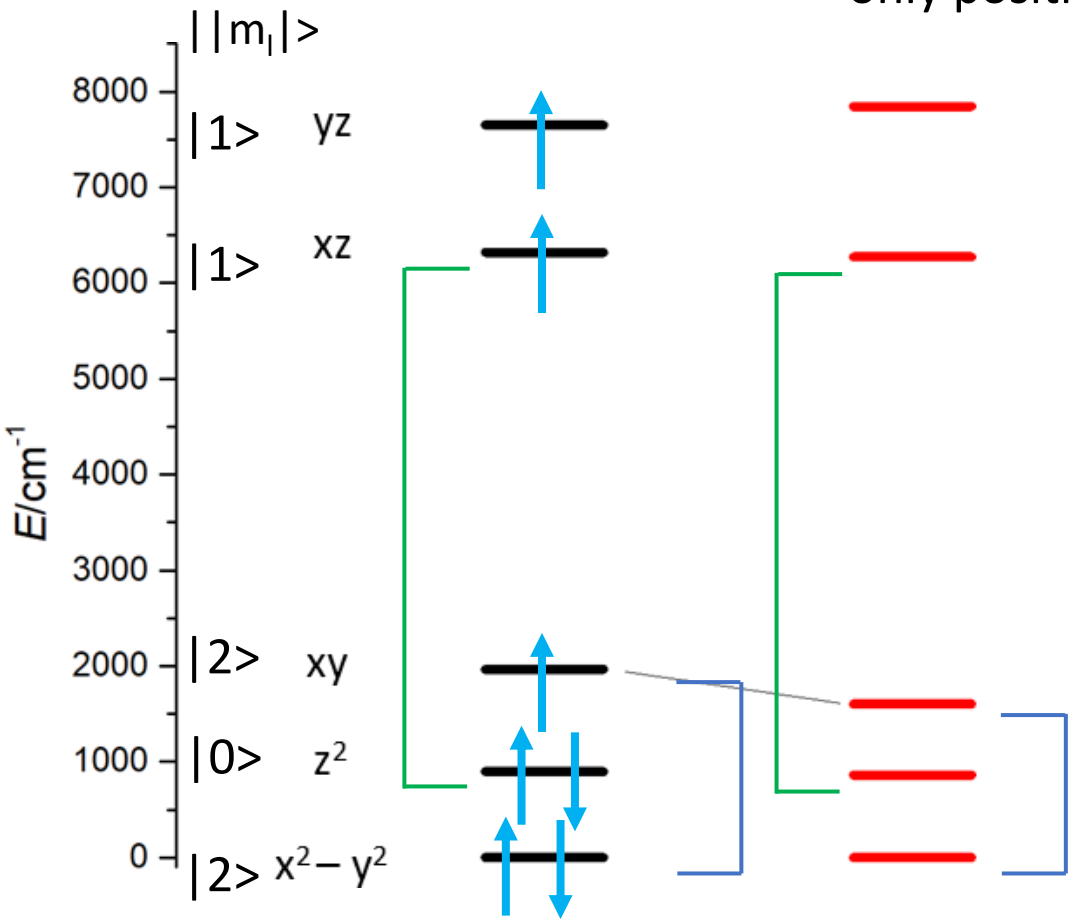

pyridine rings substituted by Ph rings

only positions of Ph rings DFT optimized

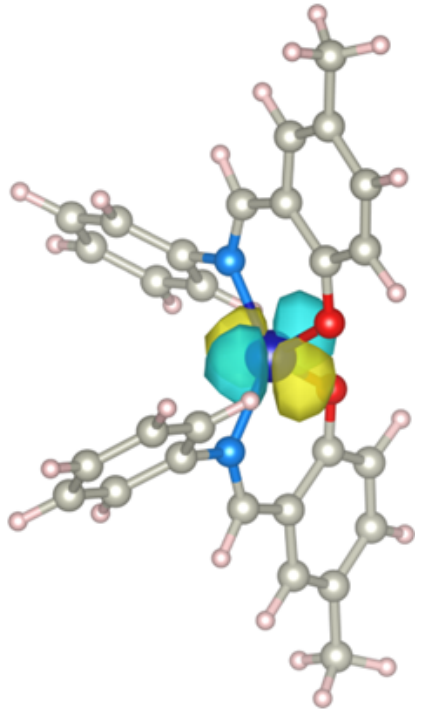

***D* = -40.1 cm^{-1}**

***E*/*D* = 0.04**

- lobes of d_{xy} points towards lone pairs of pyridine nitrogen atoms – destabilization $E(d_{xy})\uparrow$
- absence of pyridyl groups – $E(d_{xy})\downarrow$ decrease of d_{xy} energy
- lowering of d_{xy} energy leads to increase of $|D|$

S. Gomez-Coca *et al. J. Am. Chem. Soc.* **2013**, 135, 18, 7010

CASSCF/NEVPT2 calculations
All prepared complexes

c.n. 4+1 ▼

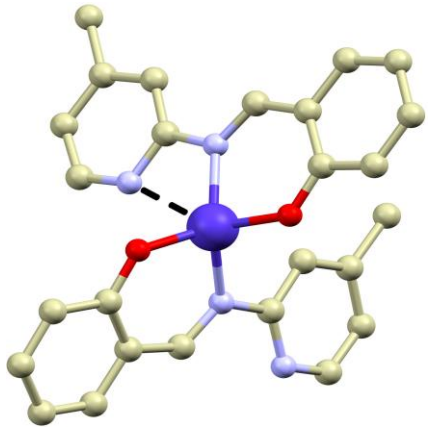

c.n. 4+2 ▼

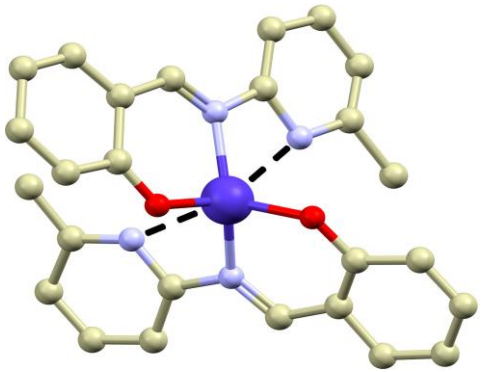

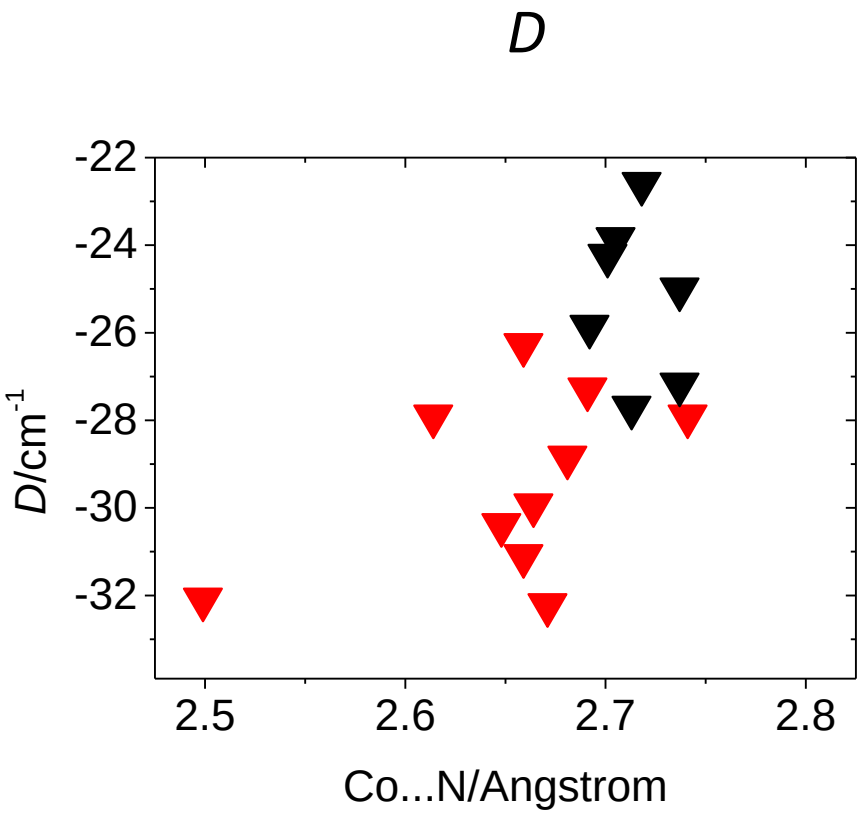

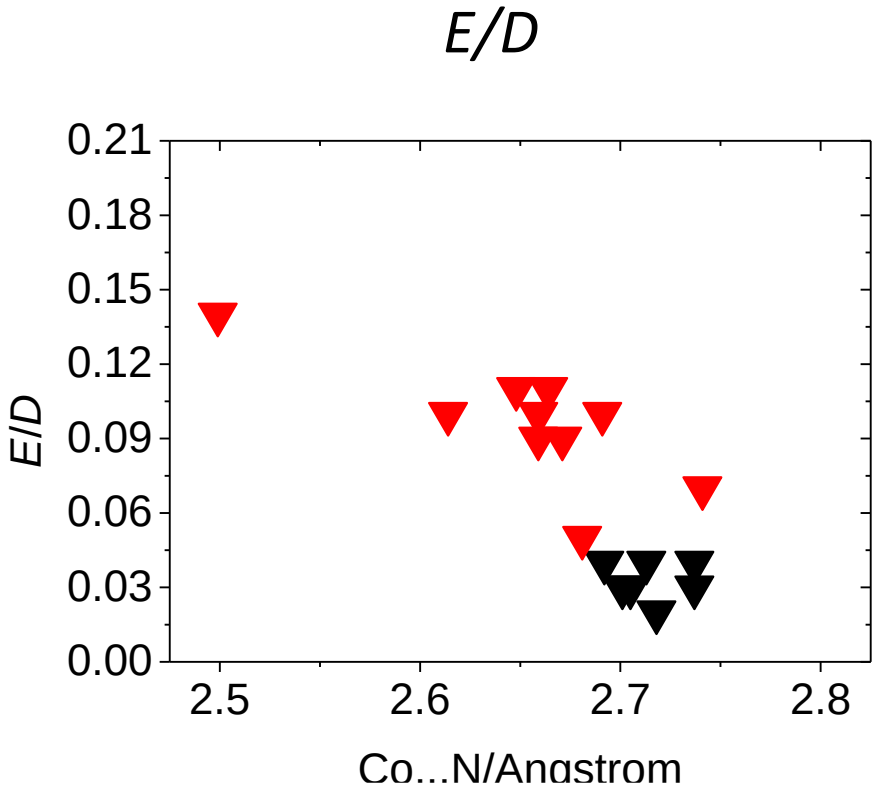

shorter Co···N contact ≈ larger $|D|$

shorter Co···N contact = larger E/D

Dynamic magnetic data

$$\frac{1}{\tau} = \frac{1}{\tau_{\text{Orbach}}} + \frac{1}{\tau_{\text{Raman}}} + \frac{1}{\tau_{\text{direct}}} + \frac{1}{\tau_{\text{QT}}}$$

$$= \frac{1}{y_0} \exp\left(-\frac{U}{k_B T}\right) + d\left(\frac{1+eH^2}{1+fH^2}\right) T^n + aH^m T + \frac{b_1}{1+b_2 H^2}$$

U_{eff} = 48.2 K, $\tau_0 = 9\times10^{-9}$s^{-1}

Ivan Šalitroš
CEITEC Brno
STU Bratislava

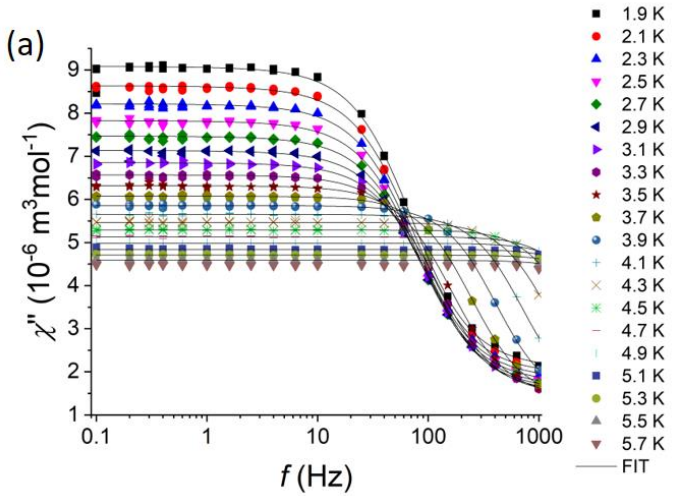

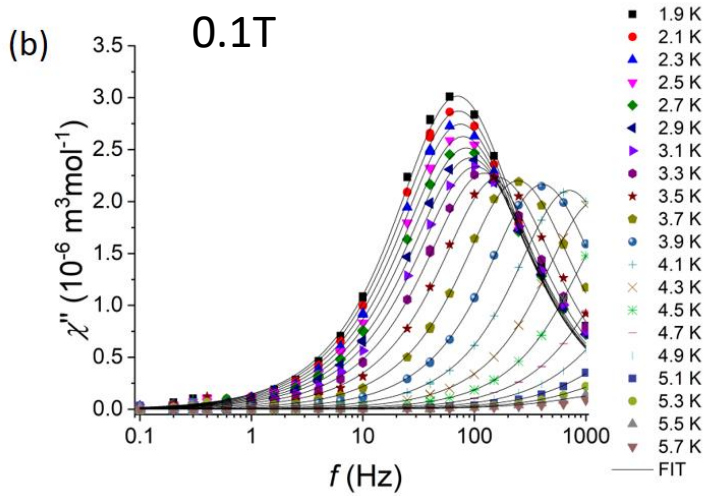

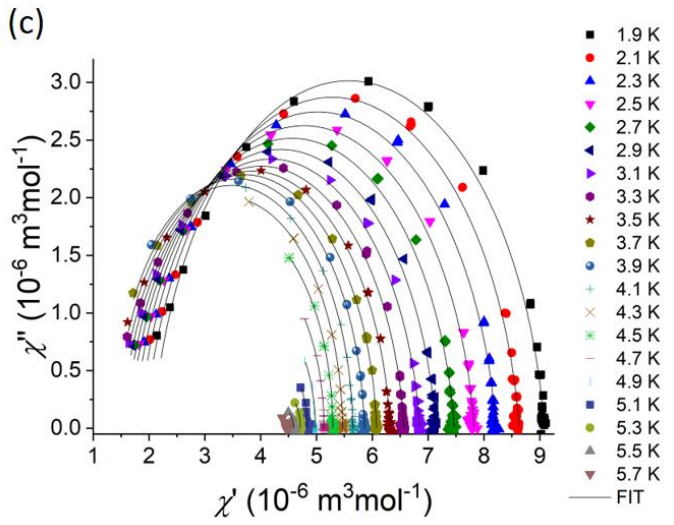

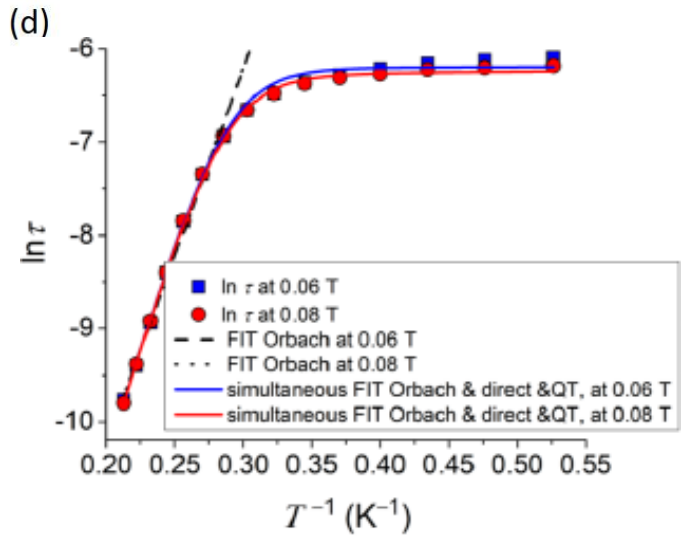

SINGLE_ANISO

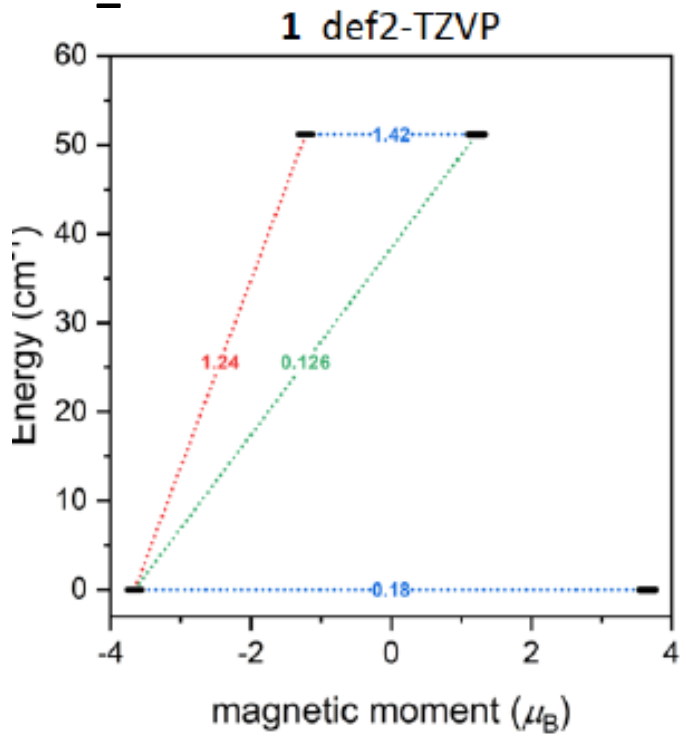

Depositions on graphene

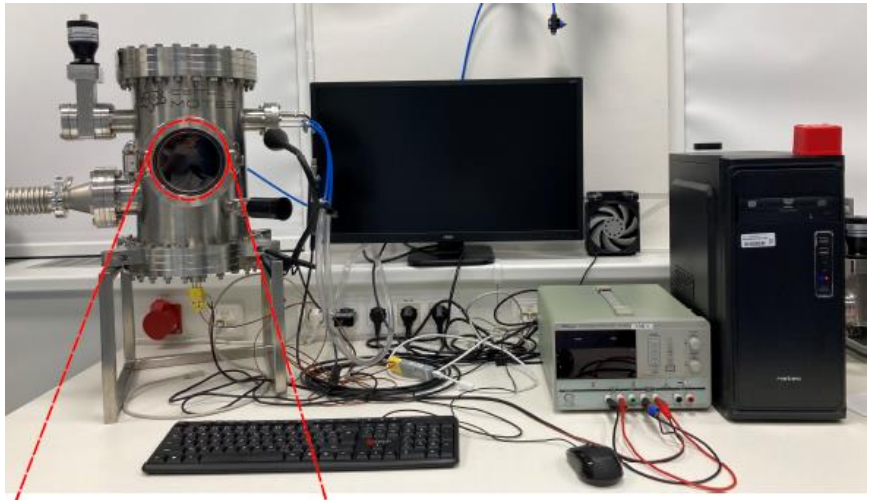

Home-built high-vacuum sublimation chamber
Base pressure: 1 x 10^{-6} mbar
•QCM for film thickness monitoring
•Heated crucible for sample
•Temperature monitoring by thermocouple

Dr. Jakub Hrubý
PhD at CEITEC Brno
currently: NHMFL, Tallahassee, USA

Šárka Vavrečková
MSc at CEITEC Brno
currently: Friedrich-Schiller Universitat Jena, Germany

Wet deposition
- From diluted solutions (drop-casting)

Characterization
- XPS
- AFM
- micro-Raman spectrocopy

Substrates used
- CVD graphene on Si/SiO_2

Depositions on graphene

1

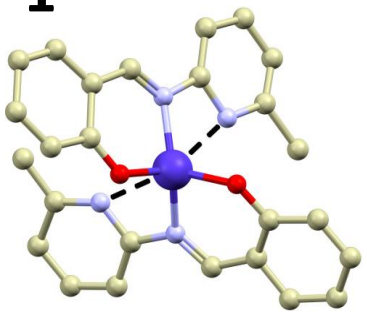

d(Co···N) = 2.6908(19) Å

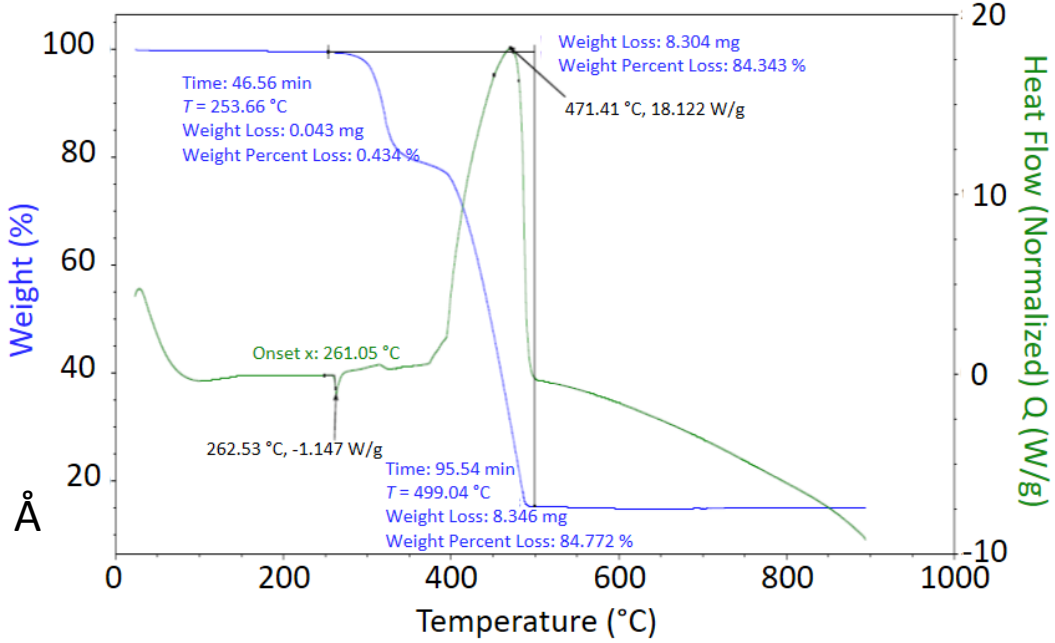

2

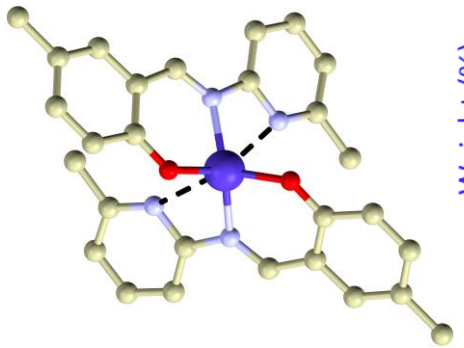

d(Co···N) = 2.6951(9) Å

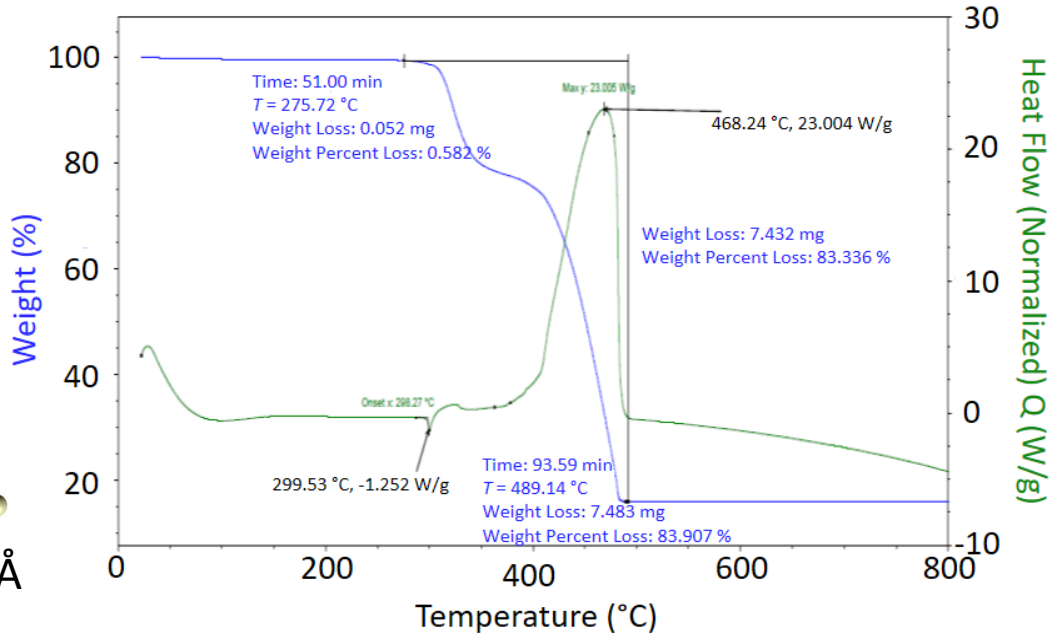

Thermal evaporation

starts of deposition were detected at 270 °C for **1** and at 283 °C for **2**.

Both compounds were thermally evaporated for 4 days.

Drop casting

A solution (*c* =1 mM) was drop-casted under ambient conditions, where 4 x 10 µL of the solution was deposited onto a substrate.

J. Navarro et al, *PCCP*. **2023**, 25, 29516

Depositions on graphene: AFM & XPS

1 Bulk

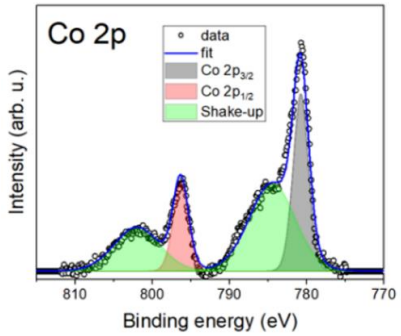

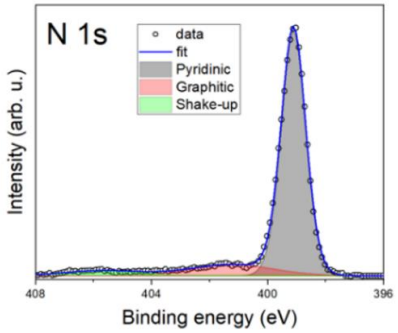

1 Thermal deposition

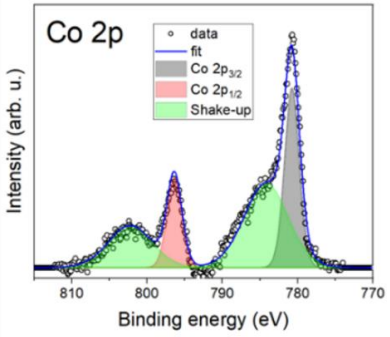

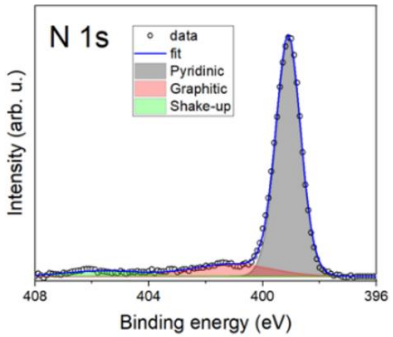

1 Drop-casting

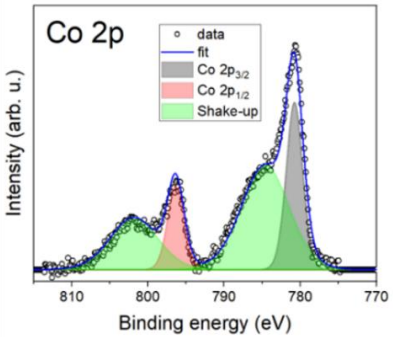

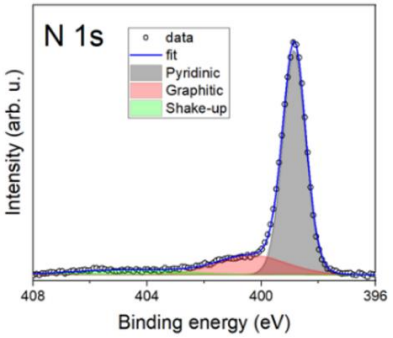

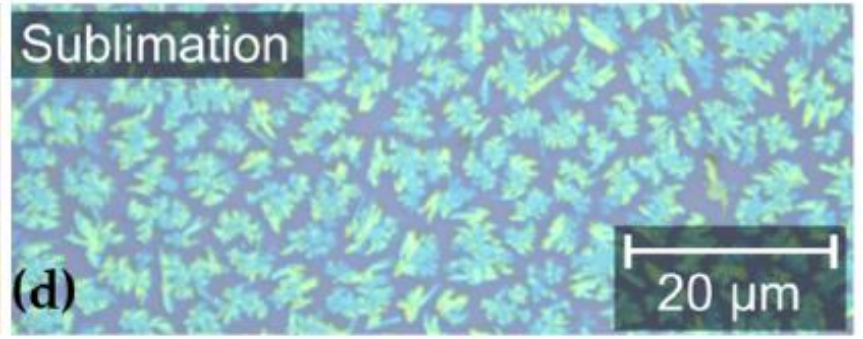

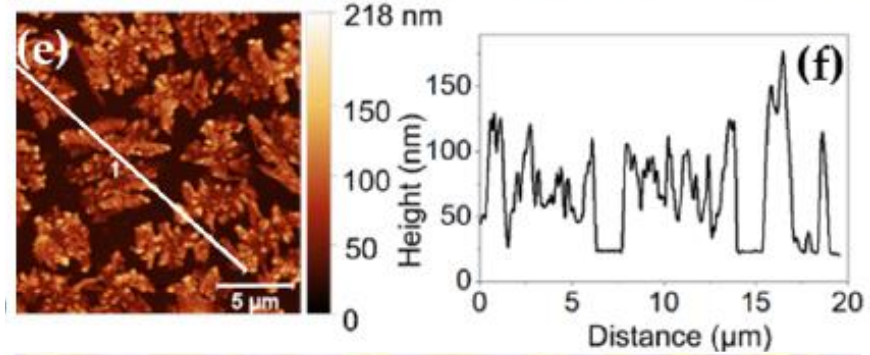

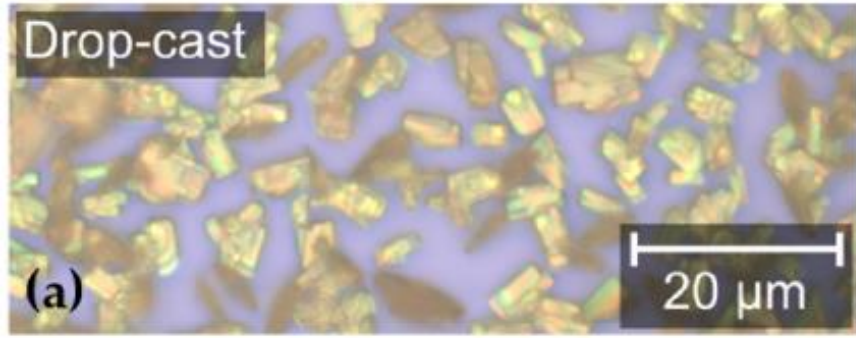

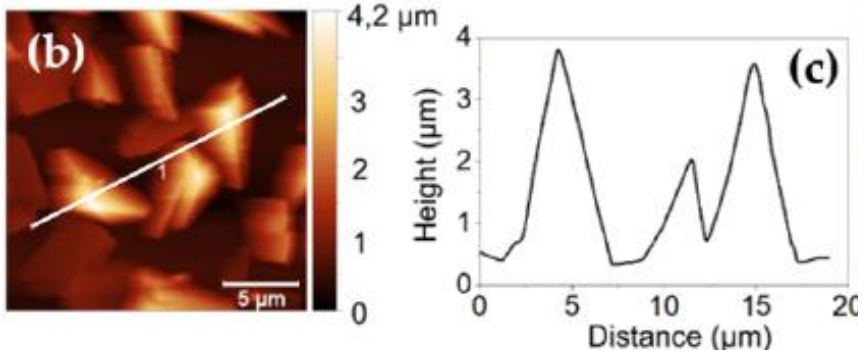

Depositions on graphene: micro-Raman

1

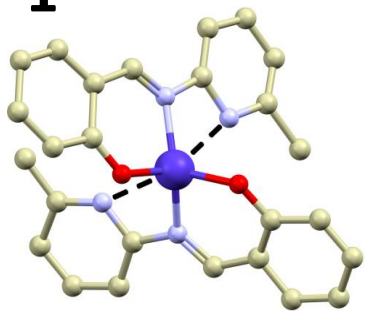

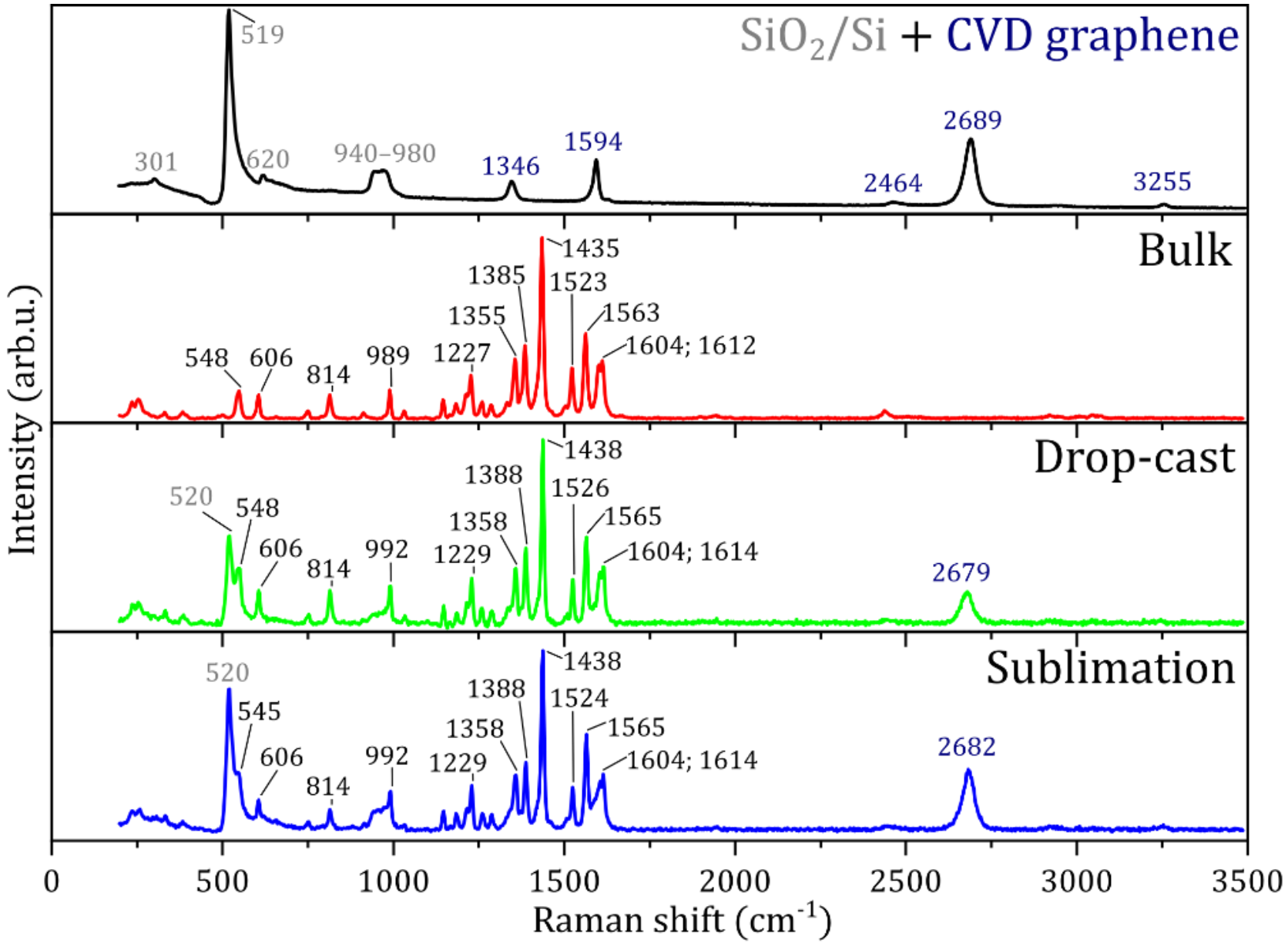

J. Navarro et al, *PCCP*. **2023**, 25, 29516

Depositions on graphene: micro-Raman

Jorge G. Navarro
CEITEC Brno

shift of graphene's 2D peak to lower *E*
→ n-doping due to deposited molecules

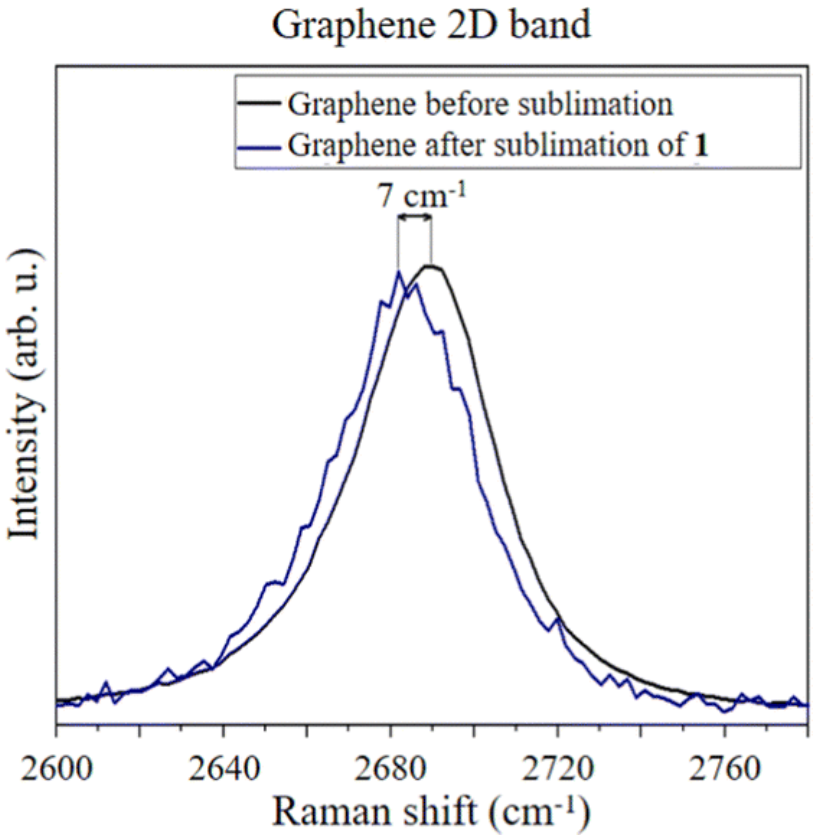

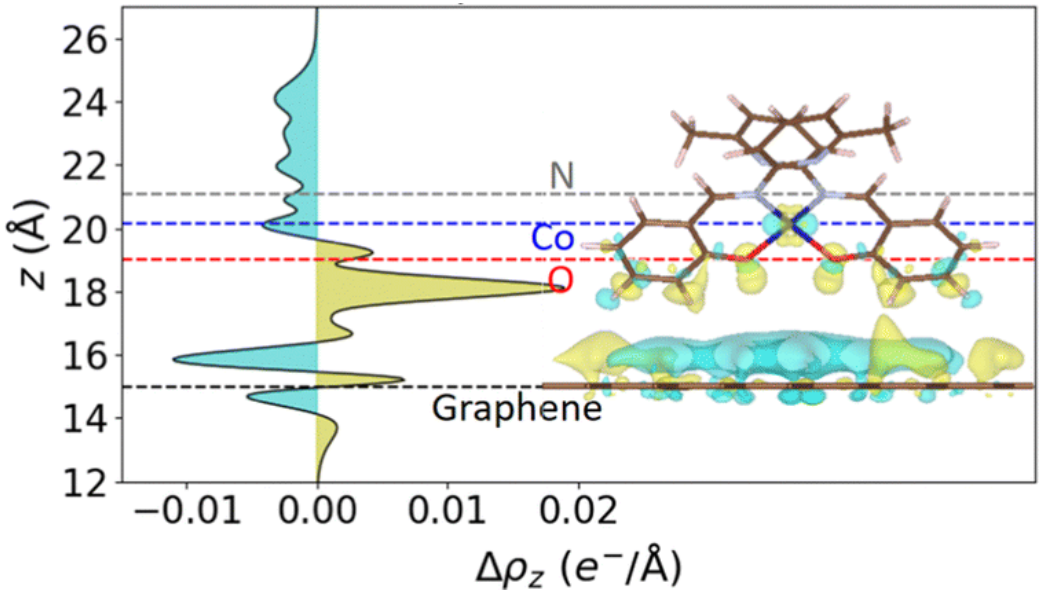

<u>DFT calculations</u>
For various conformations transfer of electrons from molecules to graphene was confirmed

consistent with n-doping

J. Navarro et al, *PCCP*. **2023**, 25, 29516

Depositions on graphene: transport measurements

- 0.1mmol solutions drop-casted on surface of graphene field-effect transistors
- gate voltage was varied from zero to 100 V
- charge neutrality point for deposited was shifted by -23V
- Electron transfer to the graphene was confirmed

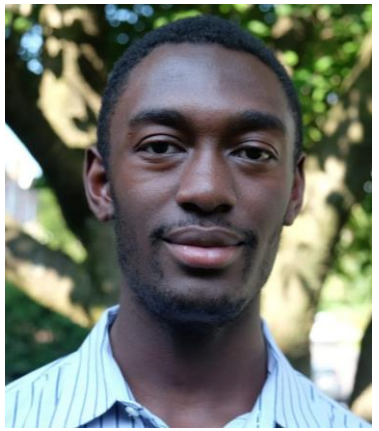

Davonne Henry & Shehan da Silva
Paola Barbara, Georgetown University

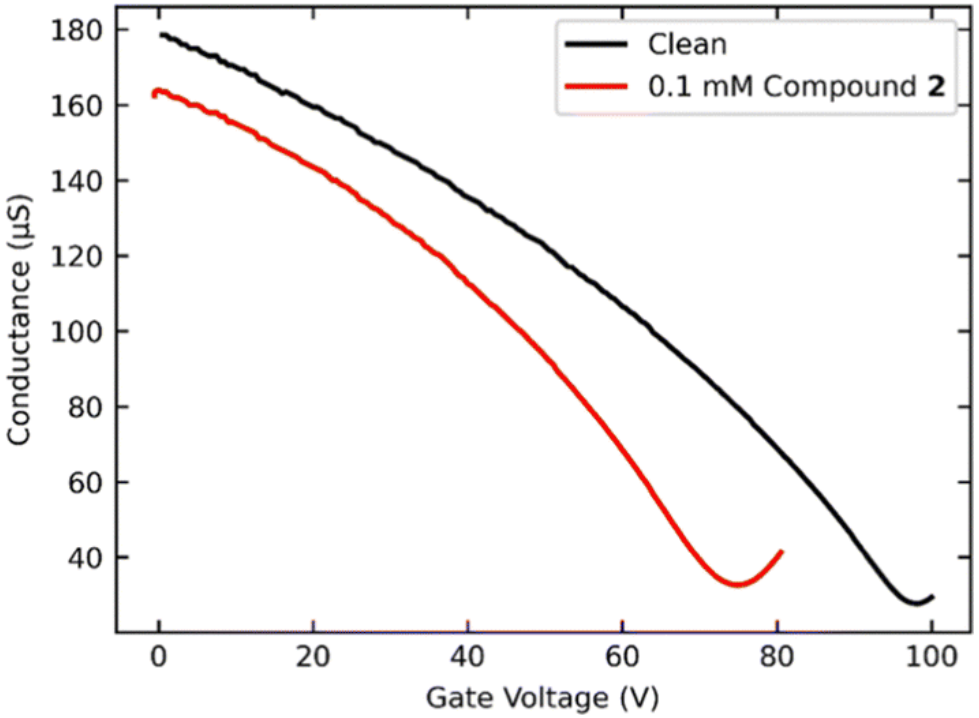

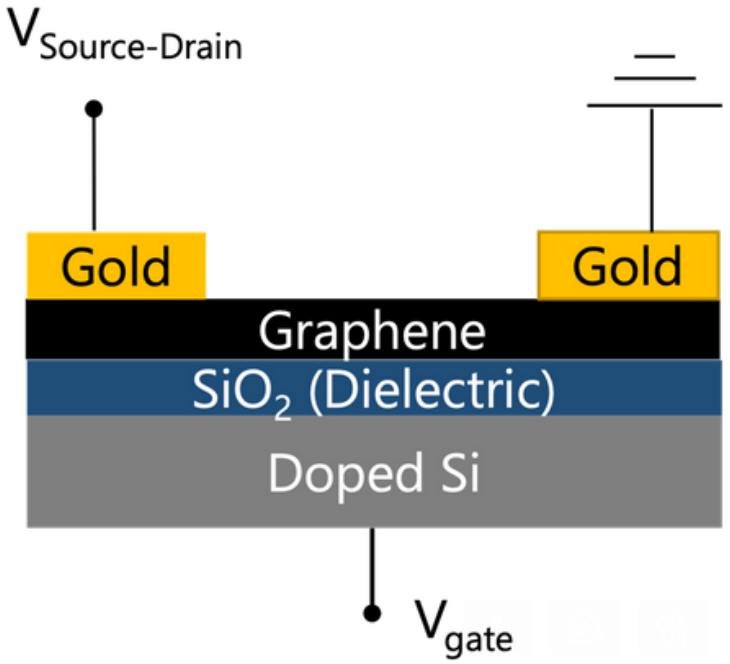

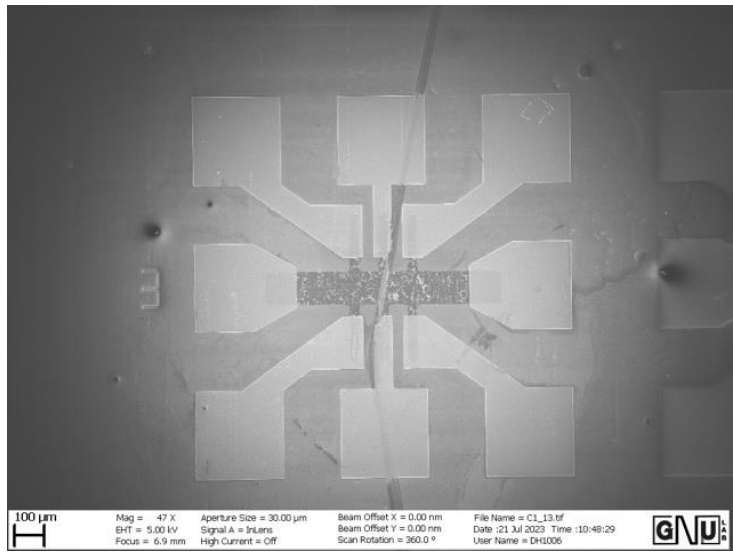

J. Navarro et al, *PCCP*. **2023**, 25, 29516

Future outlook

- utilization of semi-coordination in zero-field SMMs.

Schiff bases again

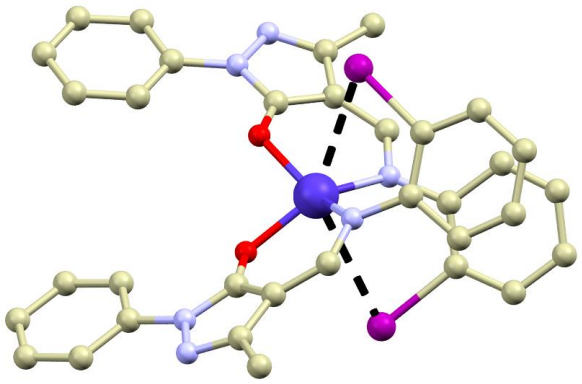

d(Co···I) = 3.28 Å

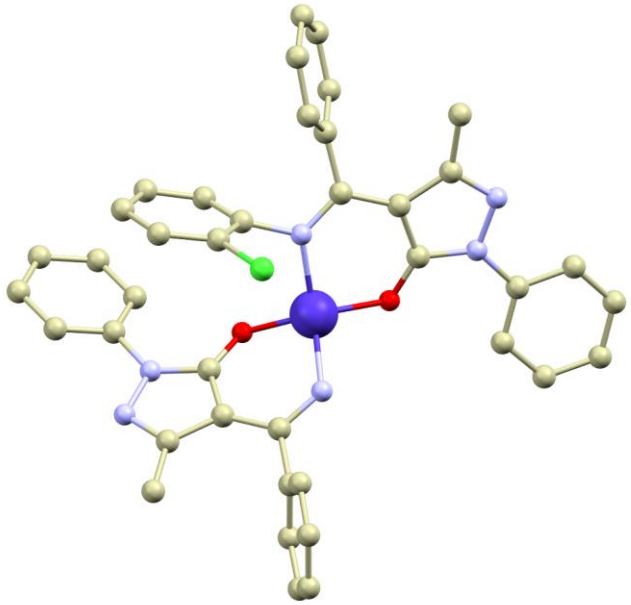

d(Co···Cl) = 3.36 Å

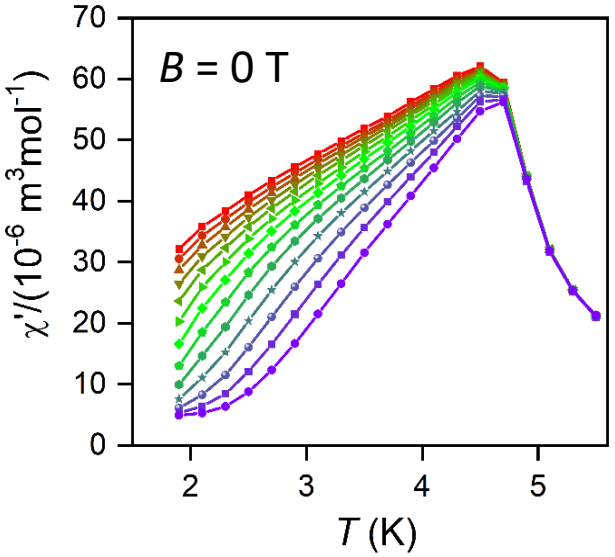

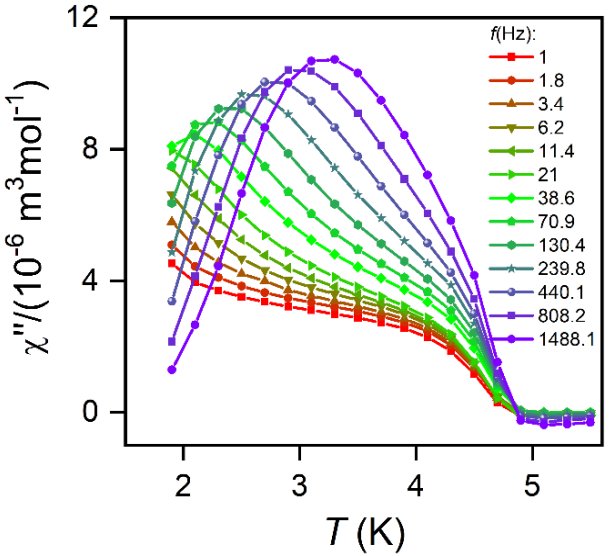

Future outlook

- utilization of semi-coordination in zero-field SMMs.

diazotation reaction

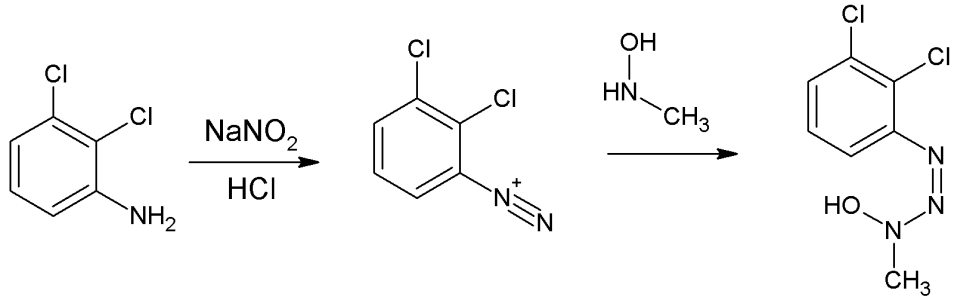

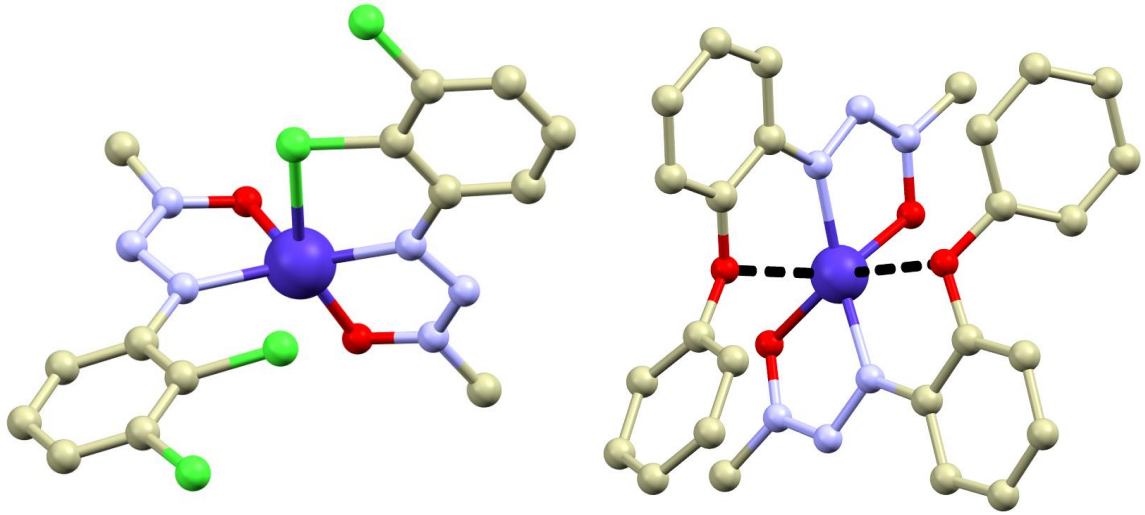

d(Co···Cl) = 2.68 Å

d(Co···O) = 2.52 and 2.73 Å

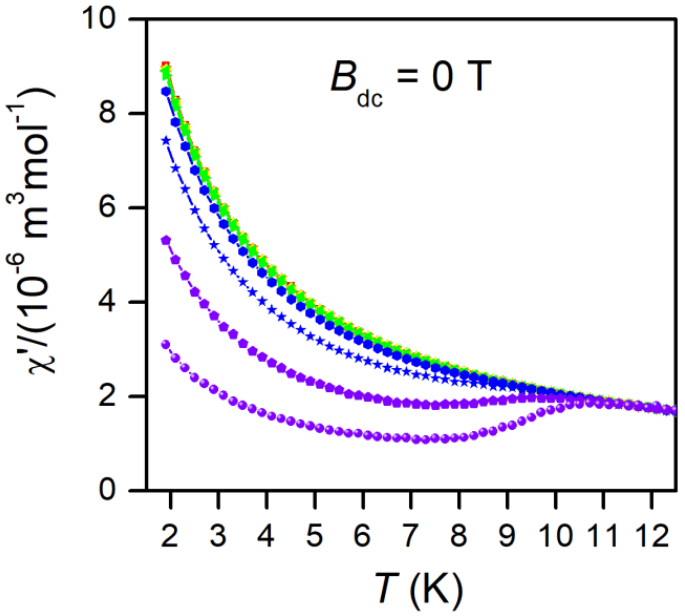

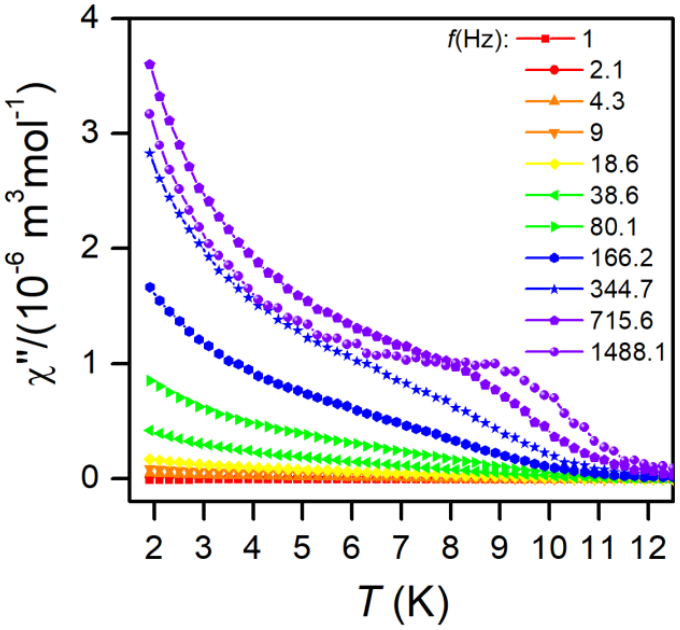

Future outlook

- utilization of semi-coordination in zero-field SMMs.

  sulfonylation reactions


Petr Halas & Ondřej F. Fellner
Palacky Uni Olomouc

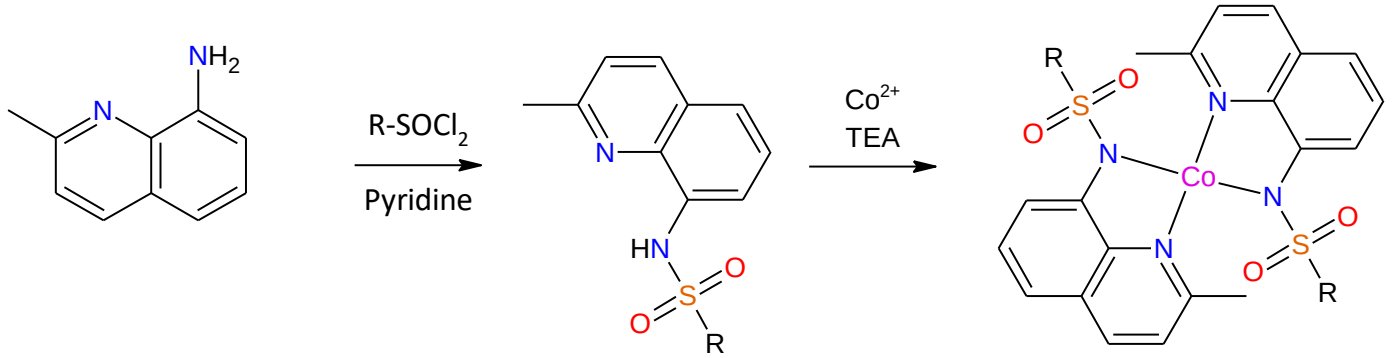

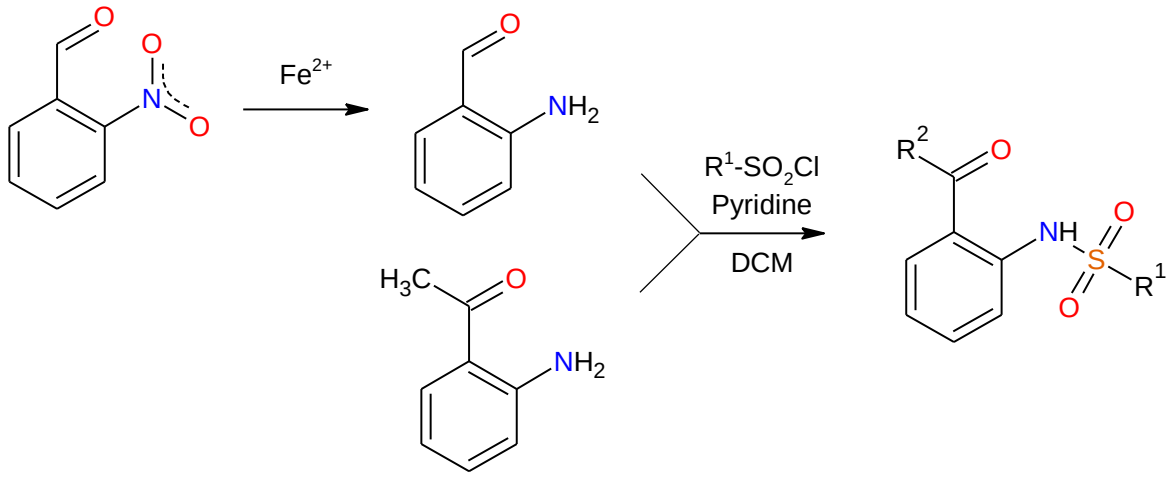

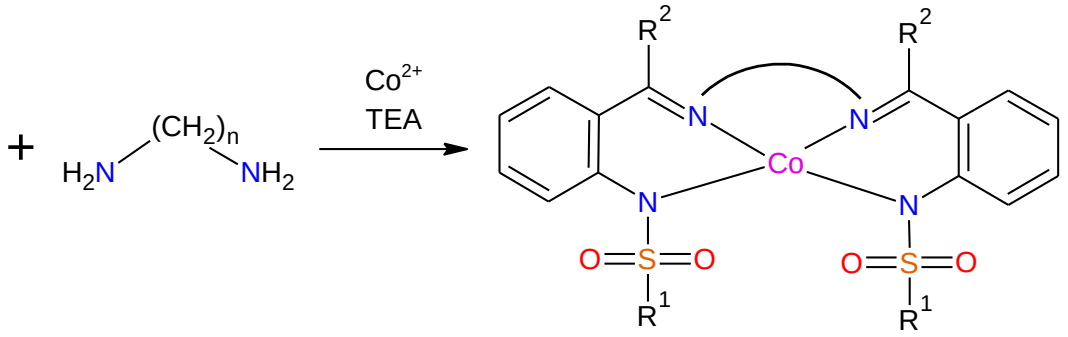

R^2 = H, CH_3

Future outlook

- utilization of semi-coordination in zero-field SMMs.

sulfonylation reactions

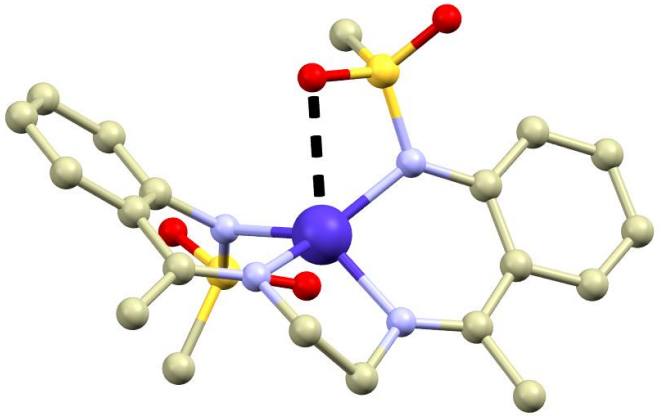

d(Co···O) = 2.69 Å
D = -125 cm^{-1}
ZF-SMM

E/Z isomerisation

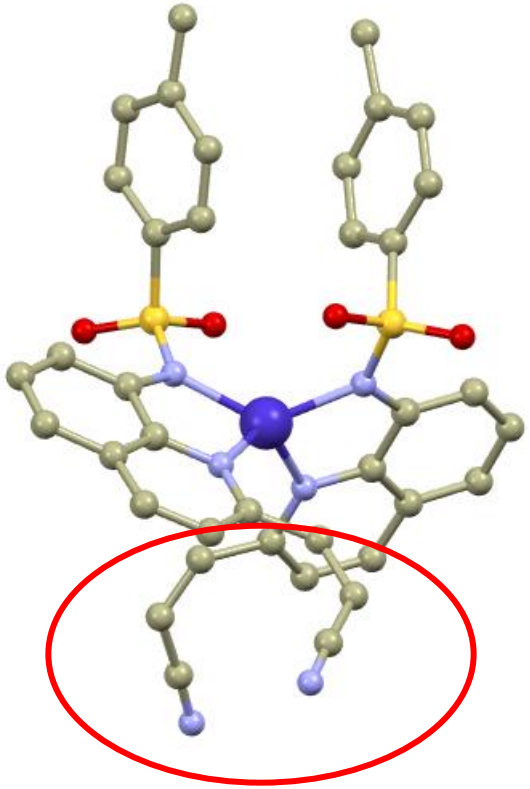

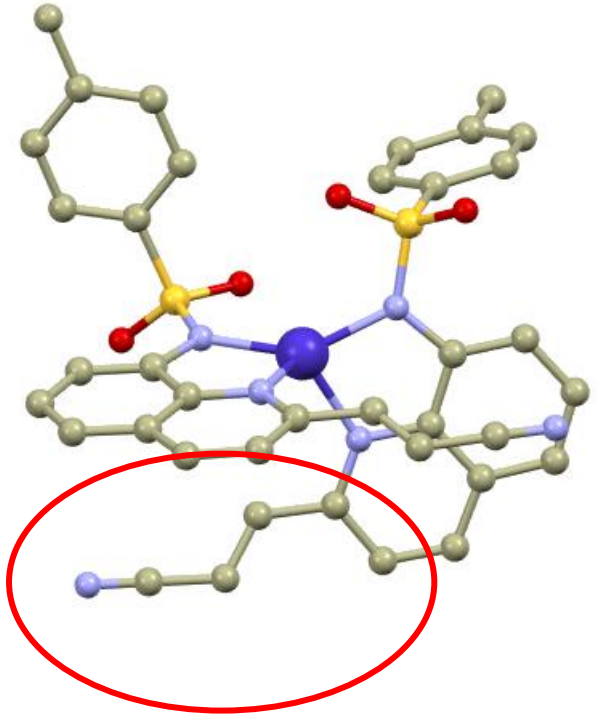

Petr Halas & Ondřej F. Fellner
Palacky Uni Olomouc

Conclusions

- We employed semi-coordination in design and synthesis of Co(II) field-induced SIMs
- We confirmed that the Co···N interactions have attractive and electrostatic nature
- We explained how the Co···N interactions influence the value of *D* parameter
- We successfully used some of the prepared complexes for deposition on the graphene by thermal evaporation

Acknowledgement

Synthesis

O.F. Fellner (UP Olomouc, CZ)
Petr Přecechtěl (UP Olomouc, CZ)
Petr Halaš (UP Olomouc, CZ)

Theoretical calculations

Radovan Herchel (UP Olomouc, CZ)

HF-EPR & Depositions

Jakub Hrubý (CEITEC Brno, CZ)
Šárka Vavrečková (CEITEC Brno, CZ)
Jorge G. Navarro (CEITEC Brno, CZ)
Vinicius T. Santana (CEITEC Brno, CZ)
Petr Neugebauer (CEITEC Brno, CZ)

SQUID magnetometry

Ivan Šalitroš (STU Bratislava, SK)
Eric McInnes (University of Manchester, UK)

Transport measurements

Davonne Henry (Georgtown University, USA)
Shenan da Silva (Georgtown University, USA)
Paola Barbara (Georgtown University, USA)

Funding

"Semicoordination: a way to chemically stable molecular nanomagnets" (Grant Agency of Czech Republic, 23-07175S)